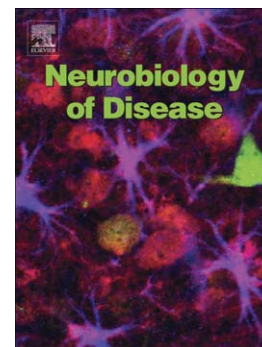# Accepted Manuscript

Mic60/mitofilin overexpression alters mitochondrial dynamics and attenuates vulnerability of dopaminergic cells to dopamine and rotenone

Victor S. Van Laar, Sarah B. Berman, Teresa G. Hastings

Please cite this article as: Van Laar, Victor S., Berman, Sarah B., Hastings, Teresa G., Mic60/mitofilin overexpression alters mitochondrial dynamics and attenuates vulnerability of dopaminergic cells to dopamine and rotenone, *Neurobiology of Disease* (2016), doi: 10.1016/j.nbd.2016.03.015

This is a PDF file of an unedited manuscript that has been accepted for publication. As a service to our customers we are providing this early version of the manuscript. The manuscript will undergo copyediting, typesetting, and review of the resulting proof before it is published in its final form. Please note that during the production process errors may be discovered which could affect the content, and all legal disclaimers that apply to the journal pertain.

Mic60/Mitofilin Overexpression Alters Mitochondrial Dynamics and Attenuates Vulnerability of Dopaminergic Cells to Dopamine and Rotenone

Victor S. Van Laar[1,3], Sarah B. Berman[1,3], and Teresa G. Hastings[1,2,3] *

Department of Neurology[1], Department of Neuroscience[2], and the Pittsburgh Institute for Neurodegenerative Diseases[3], University of Pittsburgh, Pittsburgh, Pennsylvania, U.S.A.

Running Title: Mic60 alters vulnerability of dopaminergic cells to stressors

Address Correspondence to:

* Teresa G. Hastings, Ph.D.

Pittsburgh Institute for Neurodegenerative Diseases

Department of Neurology

University of Pittsburgh School of Medicine

7038 Biomedical Science Tower 3

3501 Fifth Avenue

Pittsburgh, PA 15213

Tel: (412) 624-9716

Fax: (412) 648-7029

E-mail: hastingst@upmc.edu

ABSTRACT

Mitochondrial dysfunction has been implicated in Parkinson's disease (PD) neuropathology. Mic60, also known as mitofilin, is a protein of the inner mitochondrial membrane and a key component of the mitochondrial contact site and cristae junction organizing system (MICOS). Mic60 is critical for maintaining mitochondrial membrane structure and function. We previously demonstrated that mitochondrial Mic60 protein is susceptible to both covalent modification and loss in abundance following exposure to dopamine quinone. In this study, we utilized neuronally-differentiated SH-SY5Y and PC12 dopaminergic cell lines to examine the effects of altered Mic60 levels on mitochondrial function and cellular vulnerability in response to PD-relevant stressors. Short hairpin RNA (shRNA)-mediated knockdown of endogenous Mic60 protein in neuronal SH-SY5Y cells significantly potentiated dopamine-induced cell death, which was rescued by co-expressing shRNA-insensitive Mic60. Conversely, in PC12 and SH-SY5Y cells, Mic60 overexpression significantly attenuated both dopamine- and rotenone-induced cell death as compared to controls. Mic60 overexpression in SH-SY5Y cells was also associated with increased mitochondrial respiration, and, following rotenone exposure, increased spare respiratory capacity. Mic60 knockdown cells exhibited suppressed respiration and, following rotenone treatment, decreased spare respiratory capacity. Mic60 overexpression also affected mitochondrial fission/fusion dynamics. PC12 cells overexpressing Mic60 exhibited increased mitochondrial interconnectivity. Further, both PC12 cells and primary rat cortical neurons overexpressing Mic60 displayed suppressed mitochondrial fission and increased mitochondrial length in neurites. These results suggest that altering levels of Mic60 in dopaminergic neuronal cells significantly affects both mitochondrial homeostasis and cellular vulnerability to the PD-relevant stressors dopamine and rotenone, carrying implications for PD pathogenesis.

KEY WORDS

Mitofilin; Mic60; Parkinson's disease; mitochondria; mitochondrial dynamics; fission; fusion; rotenone; dopamine; SH-SY5Y; PC12

ABBREVIATIONS

Carbonyl cyanide-4-(trifluoromethoxy) phenylhydrazone (FCCP); dimethyl sulfoxide (DMSO); Direct Observation of Fission and Fusion (DrOF); dopamine (DA); dopamine quinone (DAQ); electron transport chain (ETC); empty vector pRS plasmid negative control TR20003 (EV-shRNA); GFP-targeted shRNA construct negative control TR30003 (GFP-shRNA); Mic60 targeted shRNA TI348605 (Mic60'05); Mic60 targeted shRNA TI348607 (Mic60'07); Mic60 targeted shRNA TI348608 (Mic60'08); mitochondrial contact site and cristae junction organizing system (MICOS); mitochondrial DNA (mtDNA); mitochondria-matrix targeted DsRed2 (mtDsRed2); mitochondria-matrix targeted photoactivatable GFP (PA-mtGFP); mitochondrially-targeted eYFP (mitoYFP); nerve growth factor (NGF); oxygen consumption rate (OCR); Parkinson's disease (PD); retinoic acid (RA); Reactive oxygen species (ROS); short-hairpin RNA (shRNA)

INTRODUCTION

Parkinson's disease (PD) is a debilitating movement disorder that results in part from the degeneration of nigrostriatal dopaminergic neurons. While the specific mechanisms responsible for initiating the disease remain elusive, evidence points to mitochondrial dysfunction as a critical factor in disease pathogenesis (Moon and Paek, 2015; Ryan et al., 2015). Maintenance and integrity of mitochondrial structure are essential to proper function and overall cellular health. In particular, the organization and shape of the inner membrane, the site of the electron transport chain (ETC) and ATP generation, are suggested to impact mitochondrial function, and may change in response to various factors (for review see: Mannella, 2006; Mannella et al., 2001; Zick et al., 2009). The mitochondrial contact site and cristae junction organizing system (MICOS) is integral in maintaining mitochondrial membrane architecture and function (Horvath et al., 2015; Pfanner et al., 2014).

MICOS is a large, multi-protein complex of the mitochondrial inner membrane, and is crucial for maintaining cristae structure, forming membrane contact sites, and protein import (Bohnert et al., 2012; Friedman et al., 2015; Harner et al., 2011; Hoppins et al., 2011; Horvath et al., 2015; Jans et al., 2013; Zerbes et al., 2012a; Zerbes et al., 2012b). A core component of the MICOS complex is the protein Mic60, also known as mitofilin (Ott et al., 2015; Pfanner et al., 2014; Zerbes et al., 2012a). Correspondingly, studies have shown that loss of Mic60 is associated with detrimental effects in mitochondrial structure and function (Bohnert et al., 2012; John et al., 2005; Li et al., 2015; Mun et al., 2010; Ott et al., 2015; Park et al., 2010; Rabl et al., 2009; von der Malsburg et al., 2011; Yang et al., 2015; Yang et al., 2012). Notably, we and others have shown that Mic60 is particularly susceptible to a loss in abundance following exposure to inducers of oxidative stress, including reactive dopamine quinones (DAQ) (Burte et al., 2011; Magi et al., 2004; Van Laar et al., 2008).

Reactive oxygen species (ROS) production and oxidative stress are associated with mitochondrial dysfunction (Schapira, 2008), and are also thought to contribute to PD neuropathology (Blesa et al., 2015). The unique susceptibility of nigrostriatal dopaminergic neurons in PD suggests that oxidative stress related to dopamine (DA) metabolism may be contributing to their degeneration

(Hastings, 2009; Hauser and Hastings, 2013; Segura-Aguilar et al., 2014; Sulzer, 2007). DA is susceptible to both enzymatic and auto-oxidation, resulting in the formation of ROS and DAQ that can covalently modify proteins (Hastings et al., 1996; Sulzer and Zecca, 2000). We have previously shown that DA oxidation products lead to mitochondrial dysfunction and the selective loss of DA terminals (Berman and Hastings, 1999; Hastings and Berman, 2000; Hastings et al., 1996; Rabinovic and Hastings, 1998; Rabinovic et al., 2000). Using proteomics techniques, we also found that specific mitochondrial proteins are susceptible to covalent modification and loss following DAQ exposure (Van Laar et al., 2008; Van Laar et al., 2009).

We discovered that Mic60 is a target for covalent modification by DAQ (Van Laar et al., 2009), potentially altering its function in MICOS. In addition, exposure of rat brain mitochondria to DAQ decreased levels of several mitochondrial proteins. Mic60 was one of the most profoundly affected proteins, decreasing in abundance by 65% following acute exposure to DAQ (Van Laar et al., 2008). Mic60 protein levels were also shown to be significantly decreased in cells following exposure to exogenous DA (Van Laar et al., 2008), the PD-associated toxin MPTP (Burte et al., 2011), and ROS-inducing photodynamic therapy (Magi et al., 2004). We hypothesize that altered Mic60 availability and function may contribute to mitochondrial dysfunction and selective neurodegeneration in PD, but this has never been examined.

Therefore, in this study, we examined the effect of Mic60 on the cellular and mitochondrial response to PD-relevant stressors. Using two neuronally-differentiated dopaminergic cell lines, cells were exposed to either exogenous DA or rotenone, a Complex I inhibitor that causes PD-like neurodegeneration in animal and cellular models (Betarbet et al., 2000; Sherer et al., 2003). We observed that decreased Mic60 expression potentiated DA-induced cell death, whereas Mic60 overexpression attenuated cell loss following both DA and rotenone exposures. Altering Mic60 protein levels also significantly affects mitochondrial respiration and mitochondrial fission/fusion dynamics. Our findings suggest that Mic60 protein levels influence both mitochondrial homeostasis and the vulnerability of dopaminergic cells to toxins. Given that levels of Mic60 are sensitive to oxidative stress (Burte et al., 2011; Magi et al., 2004; Van Laar et al., 2008), these findings may have implications for mitochondrial dysfunction in PD.

MATERIALS AND METHODS

Materials

Lipofectamine™ 2000, OptiMEM (Gibco), Dulbecco's modified Eagle medium (DMEM; Gibco), fetal bovine serum (FBS; HyClone), horse serum (HS; HyClone), 10,000 U/mL penicillin/10,000 µg/mL streptomycin (pen/strep; Gibco), and Geneticin ® (G418, cat#10131-035; Gibco) were purchased from Invitrogen (Carlsbad, CA). Rat-tail collagen was purchased from BD Bioscience (Bedford, MA), trypsin with 0.25% EDTA from Mediatech (Herndon, VA), nerve growth factor (NGF) from BD Bioscience, and rotenone from MP Biomedicals (Aurora, OH). Dimethyl sulfoxide, retinoic acid, dopamine, Trypan Blue, protease inhibitor cocktail (cat#P2714) and all chemicals for general buffers and solutions were purchased from Sigma (St. Louis, MO), unless otherwise noted.

Antibodies & Plasmids

Primary antibodies used in the following study include Mouse anti-FLAG® M2 antibody (1:500 dilution; Stratagene), Mouse anti-actin MAB1501 (1:75,000-100,000 dilution; Chemicon), Rabbit anti-MAP2 (1:1000; Millipore), and Rabbit anti-GAPDH ab9485 (1:15,000 dilution; Novus). The polyclonal "Genemed" rabbit anti-Mic60 antibody was made for our laboratory by Genemed Synthesis (San Antonio, TX) as previously described (Van Laar et al., 2008; Van Laar et al., 2009) and used for immunodetection at a 1:500 dilution. Fluorescent-conjugated secondary antibodies, goat anti-rabbit IRDye® 800 and goat anti-mouse IRDye® 680, were purchased from Li-Cor Biosciences and used at 1:5,000 - 1:10,000 dilutions. The "T3867" polyclonal rabbit anti-Mic60 antibody (1:1500) and the FLAG-tagged mouse Mic60 construct in pcDNA3 plasmid vector were generously provided by Jiping Zha, University of Texas Southwestern Medical Center at Dallas, Dallas TX (John et al, 2005). The mitochondrially-targeted eYFP protein expression construct in pcDNA3 plasmid vector (mitoYFP) was a gift from Ian J. Reynolds, University of Pittsburgh, Pittsburgh PA (Llopis et al., 1998; Rintoul et al., 2003). HuSH 29mer short hairpin RNA (shRNA) constructs against human Mic60 were purchased from OriGene Technologies (cat#TR312153), which included the empty vector pRS plasmid negative control TR20003 (EV-shRNA), the non-functional GFP-targeted shRNA construct negative control TR30003 (GFP-shRNA), and the functional human Mic60 targeted shRNA constructs, TI348605

(Mic60'05), TI348607 (Mic60'07), and TI348608 (Mic60'08). For mitochondrial morphology and dynamics analyses, cells were transfected with plasmids expressing mitochondria-matrix targeted DsRed2 (mtDsRed2; Clontech) and mitochondria-matrix targeted, photoactivatable GFP (PA-mtGFP), generously provided by Richard J. Youle, National Institute of Neurological Disease and Stroke at the National Institutes of Health, Bethesda, MD (Karbowski et al., 2004).

Transient Transfection and Treatment of Differentiated PC12 Cells

Proliferating PC12 cells, maintained in DMEM supplemented with 7% HS, 7% FBS, and 1% penicillin/streptomycin (PC12 media), were subcultured on rat-tail collagen coated 6-well plates at 1.125×10^5 cells/well and differentiated in DMEM supplemented with 1% HS, 1% FBS, 1% pen/strep, and 100 ng/mL NGF (PC12 differentiation media) for a total of 5-6 days. On day 3 of differentiation, media was removed (conditioned media) and replaced with 2.5 mL OptiMEM supplemented with 0.05 μg/mL NGF, and cells were transfected with 2 μg plasmid DNA and 6 μL Lipofectamine™ 2000 according to manufacturer's instructions. Transfection media was removed after 3.5 hrs and replaced with a 1:1 mixture of conditioned media and fresh PC12 differentiation media for 16-18 hrs, then replaced with full fresh PC12 differentiation media. Using Lipofectamine™ 2000, we typically observe an approximately 30-40% transfection rate in PC12 cells (unpublished observations). Non-transfected controls underwent the same media changes, without transfection reagents or DNA present.

On day 6 of differentiation (72 hr following transient transfection), cells were treated with either DA or rotenone. For DA toxicity experiments, media was replaced with fresh differentiating media with or without 150 μM DA and cells were incubated for 24 hrs, a concentration and time period we observed to elicit limited cell death (Dukes et al., 2008, unpublished observations). For rotenone toxicity experiments, rotenone was diluted in a 1:1 mixture of dimethyl sulfoxide (DMSO) and sterile H_2O. Cell media was replaced with fresh PC12 differentiation media with either 0.5 μM rotenone or equivalent volume of vehicle added, as previously described (Dukes et al., 2005).

Transient and stable transfection of SH-SY5Y cells and treatment

For transient transfection, human-derived SH-SY5Y neuroblastoma cells were maintained in DMEM supplemented with 10% FBS and 1% pen/strep (SH media), and were subcultured on 6-

well plates at 2 x 10^5 cells/well. The cell media was changed 48 hr after plating and supplemented with 20 µM retinoic acid (SH differentiation media) and the cells differentiated for a total of 5 days. On day 2 of differentiation, media was removed and replaced with a 1:1 mixture of OptiMEM and SH media lacking penicillin/streptomycin and supplemented with 5-10 µM retinoic acid. Cells were transfected with 2 µg plasmid DNA and 6 µL Lipofectamine™ 2000 according to manufacturer's instructions. Transfection media was removed after 3.5 hrs, and replaced with a 1:1 mixture of penicillin/streptomycin-free SH media and full SH differentiation media for 16-18 hr, and then replaced with full fresh SH differentiation media. We obtain approximately 70% transfection rate in differentiated SH-SY5Y cells using Lipofectamine™-based transfection (unpublished observations). Non-transfected controls underwent the same media changes, without transfection reagents or DNA present. On day 5 of differentiation (72 hr following transient transfection), media was replaced with fresh SH differentiating media with or without 150-250 µM DA and cells were incubated for 24 hrs.

For stable transfection and expression studies, proliferating SH-SY5Y cells, maintained in SH media, were plated at 1.5 x 10^6 cells/plate in 6cm plates. At 24 hrs after plating (~80% confluency) cells were transfected as described above using 4 µg plasmid DNA and 12 µL Lipofectamine™ 2000. Stable cells were selected by treating media with 700 µg/mL G418 for 4 days, followed by 500 µg/mL for 4 days. Proliferating stable-expression cells were maintained in SH media supplemented with 250 µg/mL G418. Cells were differentiated in SH media supplemented with 20 µM retinoic-acid for 5 days, without G418. On day 5, cells were either collected for Western blot analyses, or treated with media containing 250 µM DA for 24 hr or 0.5 µM rotenone for 48 hr, followed by analyzing cell viability. Non-transfected cells were maintained in parallel to the stable cell lines during selection, without G418, to serve as a passage-matched control.

Culture and transfection of Primary Rat Cortical Neurons

All animal procedures were approved by the Institutional Animal Care and Use Committee at the University of Pittsburgh and are in accordance with guidelines put forth by the National Institutes of Health in the Guide for the Care and Use of Laboratory Animals. Cortical neurons from E18 Sprague-Dawley rat embryos were dissected and cultured as previously described

(Arnold et al., 2011; Van Laar et al., 2011; modified from Ghosh and Greenberg, 1995) and plated onto glass-bottom MatTek dishes (MatTek Corp.). Cultures were maintained by feeding with ½ media changes every 3 days. Cortical neurons were transfected using Lipofectamine on day *in vitro* (DIV) 6 using previously described methods (Arnold et al., 2011; Van Laar et al., 2011). Neurons were co-transfected with mtDsRed2, PA-mtGFP, and either pcDNA3 empty vector or Mic60-FLAG plasmids, and maintained until imaging at 4 d following transfection.

Cell Collection and Viability Assay

Following treatment, SH-SY5Y cells were collected by 1 min exposure to 500 µL trypsin followed by force pipetting with SH media and isolated by centrifugation. PC12 cells were harvested by force pipetting, without trypsin, and isolated by centrifugation. For viability analyses, cells were resuspended in PBS and an aliquot taken for cell counting. Cell viability was determined by cell counting using the trypan blue exclusion assay. In all cases, cell viability in each treatment group was compared to its respective untreated or vehicle-treated control to determine percent cell death due to treatment. For Western blot analyses, collected cells were resuspended in lysis buffer (9 M urea, 2% w/v CHAPS, and 30 mM Tris-base, pH 8.0) with protease inhibitor cocktail. Final protein concentrations were determined by the Bradford method (Bradford, 1976).

SDS-PAGE and Western Blot Immunodetection of Select Proteins

For Western blot analyses, lysed whole-cell protein samples (25-50 µg/lane) were subjected to SDS-PAGE using 5-20% gradient gels (Hoefer ® Mighty Small II apparatus) and transferred to nitrocellulose (0.2 µm; BioRad) via a BioRad Trans-Blot ® Semi-Dry Electrophoretic Transfer system. Blots were blocked with Li-Cor blocking buffer supplemented with 0.2% w/v fat-free dry milk, and then exposed to primary antibody in blocking buffer with 0.1% Tween-20 for 16-18 hrs at 4°C. Immunoreactive bands were detected using Li-Cor IRDye secondary antibodies, and blots were imaged and quantified using a Li-Cor Odyssey imaging system coupled to Li-Cor analysis software.

Seahorse Analysis of Oxygen Consumption Rate (OCR)

The Seahorse XF96 (Seahorse Bioscience™) extracellular flux respirometer was used to measure respiration in intact differentiated SH-SY5Y cells. SH-SY5Y cells were cultured on 96-well

Seahorse XF96 analysis culture plates at 22,000 cells/well, and differentiated and transfected as described above. On day 5 of differentiation (day 3 after transfection), cells were treated with either DMSO vehicle or a 0.1 μM rotenone for 24 hr, which we have observed to be a sublethal treatment of rotenone (unpublished results). Before experiments to assess bioenergetic function were run, concentrations of oligomycin (1 μg/ml), carbonyl cyanide-4-(trifluoromethoxy) phenylhydrazone (FCCP; 0.15 μM), and rotenone (1 μM) with antimycin A (1 μM) were optimized to elicit maximal effects. The oxygen consumption rate (OCR) was determined via mitochondrial stress test, in which OCR was measured in basally respiring SH-SY5Y cells, and following injection of each oligomycin, FCCP, and rotenone with antimycin A. Three measurements were taken for each condition. For DMSO vehicle control conditions, all basal OCR measurements were within a range of 70-160 pmol O_2/min, confirming that we were operating within a linear range for respiration assessment. After respiration measurements were taken, the plates were fixed using 4% paraformaldehyde, and neuronal cells were immunostained for MAP2, using a Li-Cor IR800 goat anti-rabbit secondary. The 96-well plate was then scanned on a Li-Cor Odyssey imaging system and MAP2 immunoreactivity quantified using Li-Cor imaging software. The per-well respiration measurements were normalized to their respective MAP2 immunofluorescence intensity levels.

Mitochondrial Morphology and Direct Observation of Fission and Fusion (DrOF) Analysis

Differentiated PC12 cells were cultured on rat-tail collagen coated glass-bottom MatTek dishes (MatTek Corp.) and co-transfected, as described above, with plasmids expressing mitochondria-matrix targeted fluorescent DsRed2 protein (mtDsRed2), mitochondria-matrix targeted photoactivatable green fluorescent protein (PA-mtGFP), and either pcDNA3 empty vector or Mic60-FLAG. At 3 d after transfection, cells were imaged live using a heated stage on an Olympus FV1000 Confocal microscope, using a 60x oil-immersion objective as previously described (Arnold et al., 2011). For morphology assessment, random cells exhibiting mtDsRed2 expression were selected and cell bodies imaged. Cell images were blinded and assessed based on the morphological appearance of their mitochondria. Cells were categorized as exhibiting either short-to-medium length (truncated) tubular mitochondria or long tubular mitochondria.

DrOF analysis was carried out on NGF-differentiated PC12 cells and rat cortical neurons as previously described (Arnold et al., 2011). Cells were cultured and transfected as described above. Differentiated PC12 cells were imaged 3 d after transfection, and cortical neurons were imaged 4 d after transfection. For both differentiated PC12 and cortical neurons, distal neurites were selected for imaging. Random mitochondria, 3-6 per neurite, were selected for photoactivation by drawing a region of interest around the mitochondrion and exposing it to a brief 405nm laser pulse. Neurites were then imaged for DsRed2 and GFP fluorescence over time, one image taken every 10 sec over 15 min. Using the resulting time-lapse images, the photoactivated mitochondria were assessed for total fission and fusion events over the 15 min period, as previously described (Arnold et al., 2011). Mitochondrial lengths (μm) were determined by using the measurement tool in ImageJ (National Institutes of Health, Bethesda, MD). Images were thresholded and mitochondria were traced along their longest diameter.

Mitochondrial Interconnectivity Analysis

To assess mitochondrial fusion and interconnectivity in the cell body, differentiated PC12 cells were cultured and transfected as described above for DrOF analysis. Mitochondrial fusion/interconnection was then assessed using methods modified from Karbowski et al. (2004). Briefly, random cell bodies were identified, and imaged live using a heated stage on an Olympus FV1000 Confocal microscope using a 60x oil-immersion objective, as described above. 1-2 small regions of interest within the cell body were outlined for photoactivation via a brief 405nm laser pulse. The entire depth of the cell was imaged for DsRed2 and GFP fluorescence as z-stacks via confocal microscopy. Cells were imaged before photoactivation, immediately after photoactivation, and then at 20min, 40min, and 60min following photoactivation. GFP fluorescent intensity of the entire z-stack was quantified at each time point using Olympus Fluoview analysis software.

Statistical Analysis

For all cell viability experiments, results were analyzed by single-factor ANOVA followed by *post-hoc* Tukey's test, with equal sample sizes between groups, or Fisher's protected T-test, with unequal sample sizes. For mitochondrial respiration and interconnectivity studies, results were analyzed by Student's T-test with *post-hoc* Bonferroni correction. Morphology results were

analyzed by Chi-squared test. DrOF analysis results were analyzed using z-test of proportions with *post-hoc* Bonferroni correction. Significance was determined at p< 0.05.

RESULTS

Loss of Mic60 increases susceptibility of neuronal cells to DA-induced cell death

To evaluate whether the DA-induced decrease in Mic60 levels that we previously observed (Van Laar et al., 2008) could be contributing to neurotoxicity, we first directly asked whether reduced levels of Mic60 enhanced DA-induced toxicity of neuronal cells. We utilized RNA interference via transient expression of short hairpin RNA (shRNA) against Mic60 in a neuronally differentiated human cell line, SH-SY5Y. Dopaminergic SH-SY5Y cells were differentiated for five days with retinoic acid (RA, 20 μM), and were transiently transfected with one of five vectors in pRS plasmid: empty vector (EV-shRNA), negative control shRNA vector against GFP (GFP-shRNA), and three functional shRNA vectors against human Mic60 (shRNA'05, shRNA'07, and shRNA'08). Western blot analyses of cells collected 72 hrs following transfection confirmed a significant knockdown of total Mic60 protein by 23-30%, as compared to the EV-shRNA control (**Figure 1A,B**). Viability analyses at 4 d following transfection demonstrated that the Mic60 knockdown alone did not have an effect on basal viability as compared to EV-shRNA or GFP-shRNA transfection controls (**Fig 1C**)

We observed that this knockdown of Mic60 significantly potentiated cell death associated with exposure to exogenous DA. Transfected cells and non-transfected controls were treated at 72 hrs after transfection, with media containing 250 μM DA or with control media, for 24 hrs. DA exposure resulted in 13% percent cell death in non-transfected control cells, and 18% and 17% cell death in transfection-control EV-shRNA and GFP-shRNA cells, respectively (**Figure 1D**). DA-induced cell death was significantly increased, in a range of 1.5- to 2.2-fold, in the Mic60 knockdown cells transfected with shRNA'05 (28% cell death), shRNA'07 (27% cell death), and shRNA'08 (29% cell death), as compared to treated controls (**Figure 1D**).

We next found that the increased vulnerability to DA-induced toxicity observed with Mic60 knockdown was rescued by co-expressing an shRNA-resistant Mic60. For this experiment, we utilized a FLAG-tagged mouse Mic60 expression plasmid (Mic60-FLAG) (John et al., 2005) and the functional shRNA'05, which contained a 29-mer sequence not compatible with mouse Mic60 mRNA. Differentiated SH-SY5Y cells were co-transfected with one of three combinations of

plasmid DNA: (1) *"transfection-control"*: GFP-shRNA and pcDNA3 empty vector (GFP-shRNA+pcDNA3); (2) *"knockdown"*: pcDNA3 and shRNA'05 (shRNA'05+pcDNA3); or (3) *"rescue"*: shRNA'05 and mouse Mic60-FLAG (shRNA'05+Mic60-FLAG). Percent cell death following treatment with 250 μM DA was significantly increased by 85% in the *knockdown* cells as compared to *transfection-control* (**Figure 1E**). Co-expression of the shRNA-resistant Mic60-FLAG rescued the effects of shRNA'05 Mic60 knockdown, reducing cell death due to Mic60 knockdown by 42% (**Figure 1E**). Percent cell death in the Mic60 rescue cells was not significantly different from the DA-treated *transfection-control* (**Figure 1E**). There was no significant difference in basal viability among non-treated groups (not shown). These data demonstrate that the specific loss of Mic60 increases the vulnerability of dopaminergic cells to DA-induced toxicity.

Transient overexpression of FLAG-tagged mouse Mic60 protects against DA-induced cell death in differentiated SH-SY5Y cells

We next examined whether increased Mic60 was protective against exposure to DA in human neuron-like cells. Differentiated SH-SY5Y cells were transiently transfected with either empty vector pcDNA3 or Mic60-FLAG vectors on day two of differentiation, or left non-transfected as Control. Western blot analysis of cells collected 72 hrs after transfection confirmed the presence of the FLAG-tag associated with the exogenously expressed Mic60 (Figure 2A). The analysis also confirmed overexpression of total Mic60 in Mic60-FLAG cells (+117.9% above non-transfected Control cells), and showed no significant difference in endogenous Mic60 levels between Control and pcDNA3-transfected cells (**Figure 2A,B**).

In contrast to Mic60 knockdown, overexpression of Mic60 attenuated cellular vulnerability to DA exposure. Three days following transfection, cells were treated with 150 μM DA, 250 μM DA, or non-treated media for 24 hrs. As with the shRNA knockdown, overexpression of Mic60-FLAG did not affect basal viability in untreated cells, as compared to empty vector pcDNA3 (**Figure 2C**). Exposure to 150-250 μM DA caused cell death at 24 hr in both the empty vector pcDNA3 cells and non-transfected Control cells (**Figure 2D,E**). Levels of DA-induced cell death were significantly attenuated in the Mic60-FLAG cells, by 45-66% of treated Control and

14

pcDNA3 vector groups, at 24 hr following exposure to 150 μM DA (3.9% cell death) and 250 μM DA (11.0% cell death).

Transient Overexpression of FLAG-tagged mouse Mic60 protects against DA- and rotenone-induced toxicity in differentiated PC12 cells

As we previously observed that dopamine exposure results in decreased Mic60 levels in neuronally-differentiated PC12 cells (Van Laar et al., 2008), we next examined whether increased Mic60 was protective against PD relevant stressors in this cell line as well. NGF-differentiated PC12 cells were transiently transfected with either empty vector pcDNA3 plasmid or Mic60-FLAG, or left non-transfected as Control cells. Western blot analysis of cells collected 72 hr following transfection detected two bands immunoreactive for endogenous rat Mic60 in Control and pcDNA3 cells (**Figure 3A**). In Mic60-FLAG cells, Western blot also confirmed the presence of a third band immunoreactive for the exogenously expressed mouse Mic60 (**Figure 3A**). Quantification showed similar levels in endogenous Mic60 between Control and pcDNA3 cells, but significantly increased total Mic60 expression in Mic60-FLAG transfected cells (+64.1% as compared to Control cells) (**Figure 3B**).

We found that Mic60 overexpression significantly attenuated both DA- and rotenone-induced cell death in differentiated PC12 cells. Three days after transfection, differentiated cells were treated for 24 hrs with 150 μM DA or non-treated media, or for 48 hrs with 0.5 μM rotenone or DMSO vehicle. As in SH-SY5Y cells, transient overexpression of Mic60-FLAG did not significantly alter basal cell viability as compared to pcDNA3 in non-treated groups (not shown). Both DA and rotenone exposure elicited cell death in non-transfected Control cells and empty vector pcDNA3 cells (**Figure 3C,D**). In Mic60-FLAG cells, levels of cell death were significantly attenuated by 50-53% of treated pcDNA3 and Control groups following DA exposure (12.7% cell death), and by 43-45% of treated pcDNA3 and Control groups following rotenone (18.7% cell death) (**Figure 3C,D**).

Stable overexpression of FLAG-tagged mouse Mic60 protects against DA- and rotenone-induced cell death in neuronally differentiated cells

We next assessed whether stable, consistent overexpression of Mic60 would also be protective. SH-SY5Y cells were stably transfected with empty-vector pcDNA3 (to control for effects of transfection and stable-expression selection), mitochondrially-targeted eYFP expression vector (mitoYFP, to control for overexpressing a mitochondrial-targeted protein), or Mic60-FLAG. Stable cells were selected with and maintained in selection media as described in **Materials and Methods**. Non-transfected cells were maintained in parallel as passage-matched Control cells, to control for effects the selection process might have on cellular vulnerability to DA or rotenone. Western blot analyses of RA-differentiated stable-expressing SH-SY5Y cells showed there was no difference in endogenous Mic60 between stable-pcDNA3 cells, stable-mitoYFP cells and Control cells. In stable-Mic60-FLAG cells, total Mic60 expression was significantly increased above stable-pcDNA3 cells (+107.3%), and was associated with detection of the FLAG-tag (**Figure 4A,B**). Basal viability of differentiated cells did not vary between passage-matched non-transfected Control, stable-pcDNA3, stable-mitoYFP, and stable-Mic60-FLAG cells (**Figure 4C**).

Neuronally-differentiated SH-SY5Y cells stably overexpressing Mic60 exhibited significantly reduced levels of cell death following exposure to either DA or rotenone. Cell death was observed following 250 μM DA treatment or 0.5 μM rotenone treatment, and stable pcDNA3 and mtYFP cells did not differ in vulnerability from non-transfected Control cells (**Figure 4D,E**). Treated stable-Mic60-FLAG cells demonstrated significantly lower cell death as compared to all other groups. Levels of cell death in treated stable-Mic60-FLAG cells were attenuated by 29% of stable pcDNA3 cells following DA exposure, and by 65% of stable pcDNA3 cells following rotenone (**Figure 4D,E**). Similar results were observed in stable Mic60-overexpressing PC12 cells (**Supplementary Material**). Results from both the transient-transfected and stable-transfected cells suggest that increased Mic60 expression decreases the vulnerability of dopaminergic cells to both rotenone and exogenous DA.

Mic60 knockdown and overexpression alter basal respiration in SH-SY5Y cells, and affect mitochondrial reserve capacity in response to low-level rotenone exposure
To explore potential mechanisms of Mic60 neuroprotection, we examined the effects of Mic60 up- and down-regulation on mitochondrial function, and compared effects on respiration under

both basal and PD-relevant stress conditions. Differentiated SH-SY5Y cells expressing Mic60 shRNA or overexpressing Mic60-FLAG were assessed using a Seahorse XF96 extracellular flux respirometer to assess oxygen consumption rate (OCR) through a mitochondrial stress test.

We found that shRNA-mediated knockdown of Mic60 was associated with an impaired mitochondrial respiration capacity. Differentiated SH-SY5Y cells transfected with EV-shRNA, GFP-shRNA, or the Mic60-shRNA shRNA'08 were treated with either DMSO vehicle or 0.1 μM rotenone for 24 hr. Vehicle-treated cells transfected with shRNA'08 exhibited significantly decreased basal respiration as compared to both EV-shRNA and GFP-shRNA transfected cells, and a significantly decreased maximal respiration capacity following FCCP (uncoupled respiration) (**Figure 5A,B**). Similarly, rotenone-treated Mic60-shRNA cells exhibited a lower basal respiration and a significantly decreased maximal capacity as compared to EV-shRNA and GFP-shRNA rotenone-treated cells (**Figure 5C,D**). The spare respiratory capacity, or 'reserve capacity' (maximal respiration average – basal respiration average) was not different between vehicle-treated groups (**Figure 5E**). However, following rotenone exposure, Mic60-shRNA cells exhibited a significantly decreased reserve capacity as compared to EV-shRNA and GFP-shRNA rotenone-treated cells (**Figure 5F**).

Conversely, overexpression of Mic60 elicited an increased mitochondrial respiration capacity. Differentiated SH-SY5Y cells expressing Mic60-FLAG exhibited a significantly increased basal respiration rate as compared to pcDNA3 Empty Vector control, following 24 hr DMSO vehicle exposure (**Figure 6A,B**). Following 24 hr exposure to 0.1 μM rotenone, Mic60 overexpressing cells exhibited significantly increased basal respiration and maximal respiration rates as compared to Empty Vector (**Figure 6C,D**). While reserve capacity was not different between DMSO vehicle-treated groups (**Figure 6E**), Mic60-overexpressing cells exhibited a significantly increased reserve capacity as compared to Empty Vector following rotenone exposure (**Figure 6F**). These results suggest Mic60 expression can influence the response of the mitochondrial respiratory capacity to a stressor.

Neuronal cells overexpressing Mic60 exhibit altered mitochondrial morphology, interconnectivity, and fission/fusion dynamics

17

Previous studies have found Mic60 protein interacts, both directly and indirectly, with proteins that regulate mitochondrial dynamics, including fusion protein OPA1 and the PD-linked protein PINK1 (Abrams et al., 2015; Banerjee and Chinthapalli, 2014; Darshi et al., 2011; Weihofen et al., 2009). Because dysregulation of mitochondrial dynamics has been increasingly linked to mechanisms of degeneration in PD models (Van Laar and Berman, 2013), we investigated whether the overexpression of Mic60 influenced cellular and neuritic mitochondrial fission and fusion dynamics. NGF-differentiated PC12 cells were co-transfected with mitochondria-matrix targeted DsRed2 (mtDsRed2), mitochondria-matrix targeted photoactivatable GFP (PA-mtGFP), and either Mic60-FLAG or pcDNA3 Empty Vector, and then imaged live as described above in **Materials and Methods**.

We observed that the mitochondria of Mic60-overexpressing cells exhibited a longer, more-interconnected morphology as compared to empty vector cells (**Figure 7A,B**). We quantified cells based on the morphological appearance of their cell body mitochondria, as described above. Mic60 overexpression in PC12 cells resulted in a significant shift toward a higher proportion of cells exhibiting long tubular mitochondria as compared to Empty Vector transfected cells, which predominantly exhibited shorter-length (truncated) tubular mitochondria (**Figure 7C**).

Utilizing our direct observation of fission/fusion (DrOF) analysis (**Figure 7D**), we found that mitochondria in the neuritic projections of differentiated PC12 cells overexpressing Mic60 exhibited altered mitochondrial dynamics. Neuritic mitochondria from Mic60-overexpressing cells exhibited a significantly lower rate of fission (0.35+/-0.05 events per total photoactivated mitochondria) as compared to Empty Vector control (0.53+/-0.06 events per total photoactivated mitochondria) (**Figure 7E**). There was no significant change in fusion (**Figure 7F**). Reduced fission with unchanged fusion would result in a lower fission-to-fusion ratio, and would thus favor longer mitochondria. Correspondingly, we observed that the average length of mitochondria in PC12 neuritic projections was significantly increased in Mic60-overexpressing cells (2.47+/-0.11 μm) as compared to Empty Vector control (2.05+/-0.08 μm) (**Figure 7G).** These findings are consistent with our mitochondrial morphology data from the cell body.

We observed the same effects in the axons of cultured rat cortical neurons overexpressing Mic60. The fission rate of axonal mitochondria in Mic60-overexpressing neurons (0.29+/-0.04 events per total photoactivated mitochondria) was significantly lower as compared to Empty Vector control (0.44+/-0.05 events per total photoactivated mitochondria) (**Figure 7H**). There was no change in fusion associated with Mic60 overexpression (**Figure 7I**). We also observed that average length of neuritic mitochondria was significantly increased in Mic60-overexpressing neurons (2.26+/-0.06 μm) as compared to Empty Vector (2.04+/-0.05 μm) (**Figure 7J**), which corresponds with the lower fission-to-fusion ratio in Mic60 overexpressing neurons**.**

In addition to altered mitochondrial morphology and dynamics, differentiated PC12 cells overexpressing Mic60 displayed altered mitochondrial interconnectivity. Random cells expressing mtDsRed2, PA-mtGFP, and either pcDNA3 Empty Vector or Mic60-FLAG were chosen and select regions of mitochondria were photoactivated. The entire depth of the cell was imaged at 20 min time intervals over 1 hr (**Figure 8A,B**), and the whole-cell intensity of GFP quantified at each time point (**Figure 8C,D**). Loss in whole-cell GFP intensity over time indicates mitochondrial interconnectivity and fusion activity, as the GFP fluorescence becomes less intense due to transfer to non-photoactivated mitochondria (Karbowski et al., 2004). We found that the percent decrease in PA-mtGFP fluorescent intensity was significantly greater in Mic60 overexpressing PC12 cells at 1 hr following photoactivation (59.0+/-3.4%), as compared to Empty Vector cells (45.7+/-4.0%) (**Figure 8E**). Notably, the greatest rate of decrease for Mic60 overexpressing cells occurred within the first 20min after photoactivation, while the rate of decrease in Empty Vector cells was consistent between time points (**Figure 8F**). This suggests mitochondria were already more interconnected at the time of photoactivation in Mic60 cells as compared to Empty Vector cells. Together, these results suggest Mic60 overexpression influences basal mitochondrial dynamics, favoring decreased fission and increased connectivity.

DISCUSSION

In this study, we have demonstrated that modulation of the level of Mic60 affects the vulnerability of dopaminergic cells to two separate PD-relevant stressors, DA and rotenone. We previously observed that levels of Mic60 were decreased in an *in vitro* PD model in which cells were exposed to exogenous DA (Van Laar et al., 2008). We now show that a specific loss of Mic60 increases the vulnerability of dopaminergic neuronal cells following exposure to DA. Conversely, overexpression protects cells against DA- and rotenone-induced cell death. To our knowledge, this is the first demonstration of Mic60 overexpression improving cellular viability in response to PD-relevant stressors. We also demonstrated that Mic60 overexpression suppresses mitochondrial fission and increases mitochondrial interconnectivity. This provides functional evidence associating Mic60 with regulation of mitochondrial dynamics, corroborating previous work describing protein interactions between Mic60/MICOS and mitochondrial dynamics proteins (Abrams et al., 2015; Banerjee and Chinthapalli, 2014; Darshi et al., 2011; Weihofen et al., 2009). Given the crucial role of Mic60 in maintaining mitochondrial architecture and function, our findings carry implications for the involvement of mitochondrial structural stability in PD.

A loss of Mic60 increases vulnerability of dopaminergic cells
We found that reduction of Mic60 protein in differentiated SH-SY5Y cells was associated with a significant increase in cell death following DA exposure as compared to DA-exposed controls. Further, SH-SY5Y cells were rescued from the effect of Mic60 knockdown by transiently co-expressing a mouse Mic60 that was resistant to the shRNA. These results show that decreased Mic60 levels increase the vulnerability of dopaminergic cells to toxic insults, potentially linking the loss of Mic60 induced by DA exposure (Van Laar et al., 2008) to neuronal vulnerability. Interestingly, we only observed an effect of Mic60 loss on viability when the dopaminergic cells were exposed to PD-relevant stressors. Under control conditions, we did not observe any noticeable effect on basal viability following Mic60 knockdown in SH-SY5Y cells. This contrasts with observations of reduced mitotic growth rate and increased apoptosis in HeLa cells with reduced Mic60 (John et al., 2005; Yang et al., 2012). This could be explained by the fact that we are working with differentiated cells, examining viability at one time point.

20

Alternatively, the level of knockdown (~30%) observed in these experiments may not be dramatic enough to affect cell viability without additional stressors. It is important to note that, while high, the efficiency of our transient transfection was not 100%. Thus, it is likely the ~30% knockdown we observe is an underestimation of *individual-cell* Mic60 knockdown. Similarly, the observed increase in vulnerability of the cells to DA potentially underestimates the full effect of Mic60 loss. Nevertheless, a partial, but not complete, reduction in Mic60 may be more relevant to a chronically-stressed state as in PD, where only a portion of the total Mic60 may be oxidatively damaged at any given time. Further work will be necessary to see if modulating Mic60 levels affects basal survivability of dopaminergic cells over time.

Previous work may suggest possible mechanisms for the increased vulnerability associated with Mic60 loss. Yang et al. (2012) demonstrated that decreasing Mic60 abundance in HeLa cells resulted in a remodeling of mitochondrial cristae, correlating with increased release of cytochrome c and decreased cell viability in response to apoptosis inducers (Yang et al., 2012). Apoptotic signaling has been associated with DA-induced toxicity and cell death in SH-SY5Y dopaminergic cells (Junn and Mouradian, 2001; Zhao et al., 2007). Thus, it is possible that an increased susceptibility to cytochrome c mediated apoptosis is associated with the decreased viability we observe in Mic60-deficient SH-SY5Y cells following DA exposure.

Viability may also be affected by the rearrangement of mitochondrial cristae, impaired mitochondrial respiration, and disrupted protein import associated with Mic60 deficiency (Bohnert et al., 2012; John et al., 2005; Li et al., 2015; Rabl et al., 2009; von der Malsburg et al., 2011; Yang et al., 2015; Zerbes et al., 2012a). Here, we also show that Mic60 knockdown is associated with decreased basal respiration levels. Further, we demonstrate that rotenone exposure resulted in a significant drop in reserve respiratory capacity compared to transfection control, which suggests loss of Mic60 renders mitochondrial function more vulnerable to an oxidative phosphorylation stressor. Recent work has also found that suppressed Mic60 leads to aberrant mtDNA nucleoid formation and attenuated mtDNA transcription (Li et al., 2015; Yang et al., 2015), which would further impair mitochondrial function.

The dopaminergic profile of these cells may also be key to their susceptibility. We previously demonstrated that the production of endogenous DA in differentiated PC12 cells contributes to their vulnerability to rotenone (Dukes et al, 2005). As Mic60/mitofilin is a target for the DAQ (Van Laar et al., 2008; Van Laar et al., 2009), decreased Mic60 expression levels in dopaminergic cells may exacerbate the effects of DA-induced oxidative damage to Mic60.

Whether a specific effect or combination of effects is responsible for the influence of Mic60 loss on cellular vulnerability is unclear. Further work is necessary to elucidate the role of Mic60 in the toxin susceptibility of dopaminergic cells.

A protective role for Mic60 overexpression in the presence of stressors

We observed that increased Mic60 could attenuate cell death in response to mitochondrial stressors. Transient overexpression of FLAG-tagged Mic60 significantly decreased cell loss following exogenous DA exposure in both differentiated SH-SY5Y and PC12 cells, as well as against rotenone exposure in PC12 cells. As our transfection efficiency in these cells was not a complete 100%, it is likely that the effects of Mic60 overexpression are more profound than observed. To ensure that these were not just effects of acute overexpression, we also generated stable-expression cell lines. Stable, consistent overexpression of Mic60 was also protective against both DA and rotenone exposure in both neuronally-differentiated cell lines. Additionally, we observed no apparent effect of Mic60 overexpression, either transiently or stably expressed, on the basal viability of the cells similar to reports in other cell types (John et al., 2005). These findings suggest that excess Mic60 increases cellular tolerance against stressors, such as the PD model toxins DA and rotenone.

The DA and rotenone toxicity models have been well established in PC12 and SH-SY5Y cells, and their effects on cell viability have been attributed to factors including oxidative stress, protein modification, alterations in mitochondrial respiration and membrane potential, and mitochondrial release of apoptosis-initiating factors (Ben-Shachar et al., 2004; Berman and Hastings, 1999; Brenner-Lavie et al., 2008; Dukes et al., 2005; Imamura et al., 2006; Jones et al., 2000; Junn and Mouradian, 2001; Lai and Yu, 1997a; Lai and Yu, 1997b; Marella et al., 2007; Molina-Jimenez et al., 2003; Offen et al., 1996; Si et al., 1998; Wang et al., 2005; Watabe and

Nakaki, 2007; Zhao et al., 2007). Chronic, low-dose rotenone exposure in SH-SY5Y cells also caused decreased mitochondrial membrane potential (Sherer et al., 2001). One study found that coenzyme-Q10 supplementation reduced the effect of rotenone toxicity in SH-SY5Y cells by attenuating rotenone-induced loss of the mitochondrial membrane potential (Menke et al., 2003). Mic60, through its proposed role in mitochondrial cristae maintenance, may attenuate DA and rotenone toxicity in a similar manner by retaining mitochondrial structural integrity and respiratory capacity during cellular stress. Indeed, we observed that Mic60 overexpression boosted basal respiration, and increased spare respiratory capacity in the presence of low-dose rotenone. Similarly, Thapa et al. recently demonstrated that *in vivo* Mic60 overexpression in a transgenic mouse attenuated cardiac mitochondrial respiratory dysfunction and ROS damage in a diabetes model, possibly through preservation of mitochondrial structure (Thapa et al., 2015). Further work is necessary to elucidate the specific protective mechanisms of Mic60 overexpression in our PD models.

A role for Mic60 in neuronal mitochondrial dynamics and neurodegeneration

Our study is the first to demonstrate functional effects of Mic60 on mitochondrial dynamics in neurons and neuritic processes. Mounting evidence suggests MICOS participates in regulating mitochondrial dynamics. Previous studies have found that MICOS, and Mic60 specifically, interact with several proteins associated with mitochondrial dynamics (fusion protein OPA1, mitophagy-linked protein PINK1, and, via PINK1, the Miro/Milton mitochondrial transport complex; Abrams et al., 2015; Banerjee and Chinthapalli, 2014; Darshi et al., 2011; Weihofen et al., 2009). A recent study from Li et al. also found that loss of Mic60 was associated with reduced fission and fusion rates in mouse embryonic fibroblasts (Li et al., 2015). Our findings carry implications for the role of Mic60 in neuron health. Notably, proteins known to interact with Mic60 have been linked to neurodegenerative disorders. Mutations in the Mic60-interacting proteins OPA1 and SLC25A46 are associated with neurodegenerative optic atrophy disorders, and mutations in PINK1 cause a familial form of PD (Abrams et al., 2015; Frezza et al., 2006; Narendra et al., 2010; Wang et al., 2011). While functional interactions between these proteins and Mic60 have yet to be characterized, Mic60's interactions with proteins involved in both neurodegeneration and mitochondrial dynamics places it in a unique position to regulate cellular response to PD-relevant stress.

In this study, we observed that Mic60 overexpression suppressed mitochondrial fission rates, while not significantly affecting fusion rates. Mitochondrial fragmentation, due to increased fission and/or insufficient fusion, is associated with cell stress and apoptotic cell death (Martinou and Youle, 2011; Suen et al., 2008; Westermann, 2010). Dysregulation of mitochondrial dynamics are proposed to contribute to neurodegenerative diseases, such as PD (Burte et al., 2015; Itoh et al., 2013; Van Laar and Berman, 2013). There is evidence from multiple models to suggest that manipulating the mitochondrial fission-fusion balance can protect cellular vulnerability (Arnold et al., 2011; Reddy, 2014). In our cell culture PD models, we previously observed that chronic, low-dose rotenone induced increased fission in neurons, and inhibited neurite outgrowth in dopaminergic PC6-3 cells, a PC12 cell subclone (Arnold et al., 2011). Inhibition of fission, via dominant-negative Drp1 expression, rescued neurite outgrowth (Arnold et al., 2011). Thus, the protective effects we observe with Mic60 overexpression could be due to the associated suppression of basal fission, further suggesting that Mic60 and MICOS may be promising therapeutic targets for neurodegenerative disease.

Conclusions

We have now shown that alterations in Mic60 protein levels modulate vulnerability of two dopaminergic cell lines in two models of PD. Studies have demonstrated an integral role for Mic60 in mitochondrial functional maintenance and cristae structure organization. If Mic60 levels were altered or the protein covalently modified by a stressor, such as the oxidative DAQ, the modification could result in dissociation of mitochondrial protein import complexes and reorganization of mitochondrial cristae. This could also disrupt the interactions between Mic60 and mitochondrial dynamics proteins, interrupting regulatory effects of Mic60 complexes on mitochondrial fission/fusion. Such an event would have a major impact on mitochondrial respiration, mitochondrial homeostasis, and ultimately cellular health. The evidence provides a strong case for further study into the roles Mic60 plays in the cellular response to mitochondrial stressors. Understanding Mic60 could lead to a better knowledge of mitochondria-mediated cell death and degeneration pathways, particularly in neurodegenerative disease.

ACKNOWLEDGMENTS

BIBLIOGRAPHY

Abrams, A. J., Hufnagel, R. B., Rebelo, A., Zanna, C., Patel, N., Gonzalez, M. A., Campeanu, I. J., Griffin, L. B., Groenewald, S., Strickland, A. V., Tao, F., Speziani, F., Abreu, L., Schule, R., Caporali, L., La Morgia, C., Maresca, A., Liguori, R., Lodi, R., Ahmed, Z. M., Sund, K. L., Wang, X., Krueger, L. A., Peng, Y., Prada, C. E., Prows, C. A., Schorry, E. K., Antonellis, A., Zimmerman, H. H., Abdul-Rahman, O. A., Yang, Y., Downes, S. M., Prince, J., Fontanesi, F., Barrientos, A., Nemeth, A. H., Carelli, V., Huang, T., Zuchner, S., Dallman, J. E., 2015. Mutations in SLC25A46, encoding a UGO1-like protein, cause an optic atrophy spectrum disorder. Nat Genet. 47**,** 926-32.

Arnold, B., Cassady, S. J., VanLaar, V. S., Berman, S. B., 2011. Integrating multiple aspects of mitochondrial dynamics in neurons: age-related differences and dynamic changes in a chronic rotenone model. Neurobiol Dis. 41**,** 189-200.

Banerjee, S., Chinthapalli, B., 2014. A proteomic screen with Drosophila Opa1-like identifies Hsc70-5/Mortalin as a regulator of mitochondrial morphology and cellular homeostasis. Int J Biochem Cell Biol. 54**,** 36-48.

Ben-Shachar, D., Zuk, R., Gazawi, H., Ljubuncic, P., 2004. Dopamine toxicity involves mitochondrial complex I inhibition: implications to dopamine-related neuropsychiatric disorders. Biochem Pharmacol. 67**,** 1965-74.

Berman, S. B., Hastings, T. G., 1999. Dopamine oxidation alters mitochondrial respiration and induces permeability transition in brain mitochondria: implications for Parkinson's disease. J Neurochem. 73**,** 1127-37.

Betarbet, R., Sherer, T. B., MacKenzie, G., Garcia-Osuna, M., Panov, A. V., Greenamyre, J. T., 2000. Chronic systemic pesticide exposure reproduces features of Parkinson's disease. Nat Neurosci. 3**,** 1301-6.

Blesa, J., Trigo-Damas, I., Quiroga-Varela, A., Jackson-Lewis, V. R., 2015. Oxidative stress and Parkinson's disease. Front Neuroanat. 9**,** 91.

Bohnert, M., Wenz, L. S., Zerbes, R. M., Horvath, S. E., Stroud, D. A., von der Malsburg, K., Muller, J. M., Oeljeklaus, S., Perschil, I., Warscheid, B., Chacinska, A., Veenhuis, M., van der Klei, I. J., Daum, G., Wiedemann, N., Becker, T., Pfanner, N., van der Laan, M., 2012. Role of mitochondrial inner membrane organizing system in protein biogenesis of the mitochondrial outer membrane. Mol Biol Cell. 23**,** 3948-56.

Bradford, M. M., 1976. A rapid and sensitive method for the quantitation of microgram quantities of protein utilizing the principle of protein-dye binding. Anal Biochem. 72**,** 248-54.

Brenner-Lavie, H., Klein, E., Zuk, R., Gazawi, H., Ljubuncic, P., Ben-Shachar, D., 2008. Dopamine modulates mitochondrial function in viable SH-SY5Y cells possibly via its interaction with complex I: relevance to dopamine pathology in schizophrenia. Biochim Biophys Acta. 1777**,** 173-85.

Burte, F., Carelli, V., Chinnery, P. F., Yu-Wai-Man, P., 2015. Disturbed mitochondrial dynamics and neurodegenerative disorders. Nat Rev Neurol. 11**,** 11-24.

Burte, F., De Girolamo, L. A., Hargreaves, A. J., Billett, E. E., 2011. Alterations in the mitochondrial proteome of neuroblastoma cells in response to complex 1 inhibition. J Proteome Res. 10**,** 1974-86.

Darshi, M., Mendiola, V. L., Mackey, M. R., Murphy, A. N., Koller, A., Perkins, G. A., Ellisman, M. H., Taylor, S. S., 2011. ChChd3, an inner mitochondrial membrane protein, is essential for maintaining crista integrity and mitochondrial function. J Biol Chem. 286, 2918-32.

Dukes, A. A., Korwek, K. M., Hastings, T. G., 2005. The effect of endogenous dopamine in rotenone-induced toxicity in PC12 cells. Antioxid Redox Signal. 7, 630-8.

Dukes, A. A., Van Laar, V. S., Cascio, M., Hastings, T. G., 2008. Changes in endoplasmic reticulum stress proteins and aldolase A in cells exposed to dopamine. J Neurochem.

Frezza, C., Cipolat, S., Martins de Brito, O., Micaroni, M., Beznoussenko, G. V., Rudka, T., Bartoli, D., Polishuck, R. S., Danial, N. N., De Strooper, B., Scorrano, L., 2006. OPA1 controls apoptotic cristae remodeling independently from mitochondrial fusion. Cell. 126, 177-89.

Friedman, J. R., Mourier, A., Yamada, J., McCaffery, J. M., Nunnari, J., 2015. MICOS coordinates with respiratory complexes and lipids to establish mitochondrial inner membrane architecture. Elife. 4.

Ghosh, A., Greenberg, M. E., 1995. Calcium signaling in neurons: molecular mechanisms and cellular consequences. Science. 268, 239-47.

Harner, M., Korner, C., Walther, D., Mokranjac, D., Kaesmacher, J., Welsch, U., Griffith, J., Mann, M., Reggiori, F., Neupert, W., 2011. The mitochondrial contact site complex, a determinant of mitochondrial architecture. Embo J. 30, 4356-70.

Hastings, T. G., 2009. The role of dopamine oxidation in mitochondrial dysfunction: implications for Parkinson's disease. J Bioenerg Biomembr. 41, 469-72.

Hastings, T. G., Berman, S. B., Dopamine-Induced Toxicity and Quinone Modification of Protein: Implications for Parkinson's Disease. In: C. R. Creveling, (Ed.), Role of Catechol Quinone Species in Cellular Toxicity. FP Graham Publishing, Johnson City, TN, 2000, pp. 69-89.

Hastings, T. G., Lewis, D. A., Zigmond, M. J., 1996. Role of oxidation in the neurotoxic effects of intrastriatal dopamine injections. Proc Natl Acad Sci U S A. 93, 1956-61.

Hauser, D. N., Hastings, T. G., 2013. Mitochondrial dysfunction and oxidative stress in Parkinson's disease and monogenic parkinsonism. Neurobiol Dis. 51, 35-42.

Hoppins, S., Collins, S. R., Cassidy-Stone, A., Hummel, E., Devay, R. M., Lackner, L. L., Westermann, B., Schuldiner, M., Weissman, J. S., Nunnari, J., 2011. A mitochondrial-focused genetic interaction map reveals a scaffold-like complex required for inner membrane organization in mitochondria. J Cell Biol. 195, 323-40.

Horvath, S. E., Rampelt, H., Oeljeklaus, S., Warscheid, B., van der Laan, M., Pfanner, N., 2015. Role of membrane contact sites in protein import into mitochondria. Protein Sci. 24, 277-97.

Imamura, K., Takeshima, T., Kashiwaya, Y., Nakaso, K., Nakashima, K., 2006. D-beta-hydroxybutyrate protects dopaminergic SH-SY5Y cells in a rotenone model of Parkinson's disease. J Neurosci Res. 84, 1376-84.

Itoh, K., Nakamura, K., Iijima, M., Sesaki, H., 2013. Mitochondrial dynamics in neurodegeneration. Trends Cell Biol. 23, 64-71.

Jans, D. C., Wurm, C. A., Riedel, D., Wenzel, D., Stagge, F., Deckers, M., Rehling, P., Jakobs, S., 2013. STED super-resolution microscopy reveals an array of MINOS clusters along human mitochondria. Proc Natl Acad Sci U S A. 110, 8936-41.

John, G. B., Shang, Y., Li, L., Renken, C., Mannella, C. A., Selker, J. M., Rangell, L., Bennett, M. J., Zha, J., 2005. The mitochondrial inner membrane protein mitofilin controls cristae morphology. Mol Biol Cell. 16**,** 1543-54.

Jones, D. C., Gunasekar, P. G., Borowitz, J. L., Isom, G. E., 2000. Dopamine-induced apoptosis is mediated by oxidative stress and Is enhanced by cyanide in differentiated PC12 cells. J Neurochem. 74**,** 2296-304.

Junn, E., Mouradian, M. M., 2001. Apoptotic signaling in dopamine-induced cell death: the role of oxidative stress, p38 mitogen-activated protein kinase, cytochrome c and caspases. J Neurochem. 78**,** 374-83.

Karbowski, M., Arnoult, D., Chen, H., Chan, D. C., Smith, C. L., Youle, R. J., 2004. Quantitation of mitochondrial dynamics by photolabeling of individual organelles shows that mitochondrial fusion is blocked during the Bax activation phase of apoptosis. J Cell Biol. 164**,** 493-9.

Lai, C. T., Yu, P. H., 1997a. Dopamine- and L-beta-3,4-dihydroxyphenylalanine hydrochloride (L-Dopa)-induced cytotoxicity towards catecholaminergic neuroblastoma SH-SY5Y cells. Effects of oxidative stress and antioxidative factors. Biochem Pharmacol. 53**,** 363-72.

Lai, C. T., Yu, P. H., 1997b. R(-)-deprenyl potentiates dopamine-induced cytotoxicity toward catecholaminergic neuroblastoma SH-SY5Y cells. Toxicol Appl Pharmacol. 142**,** 186-91.

Li, H., Ruan, Y., Zhang, K., Jian, F., Hu, C., Miao, L., Gong, L., Sun, L., Zhang, X., Chen, S., Chen, H., Liu, D., Song, Z., 2015. Mic60/Mitofilin determines MICOS assembly essential for mitochondrial dynamics and mtDNA nucleoid organization. Cell Death Differ. [Epub ahead of print], doi: 10.1038/cdd.2015.102.

Llopis, J., McCaffery, J. M., Miyawaki, A., Farquhar, M. G., Tsien, R. Y., 1998. Measurement of cytosolic, mitochondrial, and Golgi pH in single living cells with green fluorescent proteins. Proc Natl Acad Sci U S A. 95**,** 6803-8.

Magi, B., Ettorre, A., Liberatori, S., Bini, L., Andreassi, M., Frosali, S., Neri, P., Pallini, V., Di Stefano, A., 2004. Selectivity of protein carbonylation in the apoptotic response to oxidative stress associated with photodynamic therapy: a cell biochemical and proteomic investigation. Cell Death Differ. 11**,** 842-52.

Mannella, C. A., 2006. The relevance of mitochondrial membrane topology to mitochondrial function. Biochim Biophys Acta. 1762**,** 140-7.

Mannella, C. A., Pfeiffer, D. R., Bradshaw, P. C., Moraru, II, Slepchenko, B., Loew, L. M., Hsieh, C. E., Buttle, K., Marko, M., 2001. Topology of the mitochondrial inner membrane: dynamics and bioenergetic implications. IUBMB Life. 52**,** 93-100.

Marella, M., Seo, B. B., Matsuno-Yagi, A., Yagi, T., 2007. Mechanism of cell death caused by complex I defects in a rat dopaminergic cell line. J Biol Chem. 282**,** 24146-56.

Martinou, J. C., Youle, R. J., 2011. Mitochondria in apoptosis: Bcl-2 family members and mitochondrial dynamics. Dev Cell. 21**,** 92-101.

Menke, T., Gille, G., Reber, F., Janetzky, B., Andler, W., Funk, R. H., Reichmann, H., 2003. Coenzyme Q10 reduces the toxicity of rotenone in neuronal cultures by preserving the mitochondrial membrane potential. Biofactors. 18**,** 65-72.

Molina-Jimenez, M. F., Sanchez-Reus, M. I., Benedi, J., 2003. Effect of fraxetin and myricetin on rotenone-induced cytotoxicity in SH-SY5Y cells: comparison with N-acetylcysteine. Eur J Pharmacol. 472**,** 81-7.

Moon, H. E., Paek, S. H., 2015. Mitochondrial Dysfunction in Parkinson's Disease. Exp Neurobiol. 24, 103-16.

Mun, J. Y., Lee, T. H., Kim, J. H., Yoo, B. H., Bahk, Y. Y., Koo, H. S., Han, S. S., 2010. Caenorhabditis elegans mitofilin homologs control the morphology of mitochondrial cristae and influence reproduction and physiology. J Cell Physiol. 224, 748-56.

Narendra, D. P., Jin, S. M., Tanaka, A., Suen, D. F., Gautier, C. A., Shen, J., Cookson, M. R., Youle, R. J., 2010. PINK1 is selectively stabilized on impaired mitochondria to activate Parkin. PLoS Biol. 8, e1000298.

Offen, D., Ziv, I., Sternin, H., Melamed, E., Hochman, A., 1996. Prevention of dopamine-induced cell death by thiol antioxidants: possible implications for treatment of Parkinson's disease. Exp Neurol. 141, 32-9.

Ott, C., Dorsch, E., Fraunholz, M., Straub, S., Kozjak-Pavlovic, V., 2015. Detailed analysis of the human mitochondrial contact site complex indicate a hierarchy of subunits. PLoS ONE. 10, e0120213.

Park, Y. U., Jeong, J., Lee, H., Mun, J. Y., Kim, J. H., Lee, J. S., Nguyen, M. D., Han, S. S., Suh, P. G., Park, S. K., 2010. Disrupted-in-schizophrenia 1 (DISC1) plays essential roles in mitochondria in collaboration with Mitofilin. Proc Natl Acad Sci U S A. 107, 17785-90.

Pfanner, N., van der Laan, M., Amati, P., Capaldi, R. A., Caudy, A. A., Chacinska, A., Darshi, M., Deckers, M., Hoppins, S., Icho, T., Jakobs, S., Ji, J., Kozjak-Pavlovic, V., Meisinger, C., Odgren, P. R., Park, S. K., Rehling, P., Reichert, A. S., Sheikh, M. S., Taylor, S. S., Tsuchida, N., van der Bliek, A. M., van der Klei, I. J., Weissman, J. S., Westermann, B., Zha, J., Neupert, W., Nunnari, J., 2014. Uniform nomenclature for the mitochondrial contact site and cristae organizing system. J Cell Biol. 204, 1083-6.

Rabinovic, A. D., Hastings, T. G., 1998. Role of endogenous glutathione in the oxidation of dopamine. J Neurochem. 71, 2071-8.

Rabinovic, A. D., Lewis, D. A., Hastings, T. G., 2000. Role of oxidative changes in the degeneration of dopamine terminals after injection of neurotoxic levels of dopamine. Neuroscience. 101, 67-76.

Rabl, R., Soubannier, V., Scholz, R., Vogel, F., Mendl, N., Vasiljev-Neumeyer, A., Korner, C., Jagasia, R., Keil, T., Baumeister, W., Cyrklaff, M., Neupert, W., Reichert, A. S., 2009. Formation of cristae and crista junctions in mitochondria depends on antagonism between Fcj1 and Su e/g. J Cell Biol. 185, 1047-63.

Reddy, P. H., 2014. Inhibitors of mitochondrial fission as a therapeutic strategy for diseases with oxidative stress and mitochondrial dysfunction. J Alzheimers Dis. 40, 245-56.

Rintoul, G. L., Filiano, A. J., Brocard, J. B., Kress, G. J., Reynolds, I. J., 2003. Glutamate decreases mitochondrial size and movement in primary forebrain neurons. J Neurosci. 23, 7881-8.

Ryan, B. J., Hoek, S., Fon, E. A., Wade-Martins, R., 2015. Mitochondrial dysfunction and mitophagy in Parkinson's: from familial to sporadic disease. Trends Biochem Sci. 40, 200-10.

Schapira, A. H., 2008. Mitochondria in the aetiology and pathogenesis of Parkinson's disease. Lancet Neurol. 7, 97-109.

Segura-Aguilar, J., Paris, I., Munoz, P., Ferrari, E., Zecca, L., Zucca, F. A., 2014. Protective and toxic roles of dopamine in Parkinson's disease. J Neurochem. 129, 898-915.

Sherer, T. B., Betarbet, R., Testa, C. M., Seo, B. B., Richardson, J. R., Kim, J. H., Miller, G. W., Yagi, T., Matsuno-Yagi, A., Greenamyre, J. T., 2003. Mechanism of toxicity in rotenone models of Parkinson's disease. J Neurosci. 23, 10756-64.

Sherer, T. B., Trimmer, P. A., Borland, K., Parks, J. K., Bennett, J. P., Jr., Tuttle, J. B., 2001. Chronic reduction in complex I function alters calcium signaling in SH-SY5Y neuroblastoma cells. Brain Res. 891, 94-105.

Si, F., Ross, G. M., Shin, S. H., 1998. Glutathione protects PC12 cells from ascorbate- and dopamine-induced apoptosis. Exp Brain Res. 123, 263-8.

Suen, D. F., Norris, K. L., Youle, R. J., 2008. Mitochondrial dynamics and apoptosis. Genes Dev. 22, 1577-90.

Sulzer, D., 2007. Multiple hit hypotheses for dopamine neuron loss in Parkinson's disease. Trends Neurosci. 30, 244-50.

Sulzer, D., Zecca, L., 2000. Intraneuronal dopamine-quinone synthesis: a review. Neurotox Res. 1, 181-95.

Thapa, D., Nichols, C. E., Lewis, S. E., Shepherd, D. L., Jagannathan, R., Croston, T. L., Tveter, K. J., Holden, A. A., Baseler, W. A., Hollander, J. M., 2015. Transgenic overexpression of mitofilin attenuates diabetes mellitus-associated cardiac and mitochondria dysfunction. J Mol Cell Cardiol. 79, 212-23.

Van Laar, V. S., Arnold, B., Cassady, S. J., Chu, C. T., Burton, E. A., Berman, S. B., 2011. Bioenergetics of neurons inhibit the translocation response of Parkin following rapid mitochondrial depolarization. Hum Mol Genet. 20, 927-40.

Van Laar, V. S., Berman, S. B., 2013. The interplay of neuronal mitochondrial dynamics and bioenergetics: implications for Parkinson's disease. Neurobiol Dis. 51, 43-55.

Van Laar, V. S., Dukes, A. A., Cascio, M., Hastings, T. G., 2008. Proteomic analysis of rat brain mitochondria following exposure to dopamine quinone: implications for Parkinson disease. Neurobiol Dis. 29, 477-89.

Van Laar, V. S., Mishizen, A. J., Cascio, M., Hastings, T. G., 2009. Proteomic identification of dopamine-conjugated proteins from isolated rat brain mitochondria and SH-SY5Y cells. Neurobiol Dis. 34, 487-500.

von der Malsburg, K., Muller, J. M., Bohnert, M., Oeljeklaus, S., Kwiatkowska, P., Becker, T., Loniewska-Lwowska, A., Wiese, S., Rao, S., Milenkovic, D., Hutu, D. P., Zerbes, R. M., Schulze-Specking, A., Meyer, H. E., Martinou, J. C., Rospert, S., Rehling, P., Meisinger, C., Veenhuis, M., Warscheid, B., van der Klei, I. J., Pfanner, N., Chacinska, A., van der Laan, M., 2011. Dual role of mitofilin in mitochondrial membrane organization and protein biogenesis. Dev Cell. 21, 694-707.

Wang, G., Qi, C., Fan, G. H., Zhou, H. Y., Chen, S. D., 2005. PACAP protects neuronal differentiated PC12 cells against the neurotoxicity induced by a mitochondrial complex I inhibitor, rotenone. FEBS Lett. 579, 4005-11.

Wang, X., Winter, D., Ashrafi, G., Schlehe, J., Wong, Y. L., Selkoe, D., Rice, S., Steen, J., LaVoie, M. J., Schwarz, T. L., 2011. PINK1 and Parkin target Miro for phosphorylation and degradation to arrest mitochondrial motility. Cell. 147, 893-906.

Watabe, M., Nakaki, T., 2007. ATP depletion does not account for apoptosis induced by inhibition of mitochondrial electron transport chain in human dopaminergic cells. Neuropharmacology. 52, 536-41.

Weihofen, A., Thomas, K. J., Ostaszewski, B. L., Cookson, M. R., Selkoe, D. J., 2009. Pink1 forms a multiprotein complex with Miro and Milton, linking Pink1 function to mitochondrial trafficking. Biochemistry. 48, 2045-52.

Westermann, B., 2010. Mitochondrial fusion and fission in cell life and death. Nat Rev Mol Cell Biol. 11, 872-84.

Yang, R. F., Sun, L. H., Zhang, R., Zhang, Y., Luo, Y. X., Zheng, W., Zhang, Z. Q., Chen, H. Z., Liu, D. P., 2015. Suppression of Mic60 compromises mitochondrial transcription and oxidative phosphorylation. Sci Rep. 5, 7990.

Yang, R. F., Zhao, G. W., Liang, S. T., Zhang, Y., Sun, L. H., Chen, H. Z., Liu, D. P., 2012. Mitofilin regulates cytochrome c release during apoptosis by controlling mitochondrial cristae remodeling. Biochem Biophys Res Commun. 428, 93-8.

Zerbes, R. M., Bohnert, M., Stroud, D. A., von der Malsburg, K., Kram, A., Oeljeklaus, S., Warscheid, B., Becker, T., Wiedemann, N., Veenhuis, M., van der Klei, I. J., Pfanner, N., van der Laan, M., 2012a. Role of MINOS in mitochondrial membrane architecture: cristae morphology and outer membrane interactions differentially depend on mitofilin domains. J Mol Biol. 422, 183-91.

Zerbes, R. M., van der Klei, I. J., Veenhuis, M., Pfanner, N., van der Laan, M., Bohnert, M., 2012b. Mitofilin complexes: conserved organizers of mitochondrial membrane architecture. Biol Chem. 393, 1247-61.

Zhao, D. L., Zou, L. B., Lin, S., Shi, J. G., Zhu, H. B., 2007. Anti-apoptotic effect of esculin on dopamine-induced cytotoxicity in the human neuroblastoma SH-SY5Y cell line. Neuropharmacology. 53, 724-32.

Zick, M., Rabl, R., Reichert, A. S., 2009. Cristae formation-linking ultrastructure and function of mitochondria. Biochim Biophys Acta. 1793, 5-19.

FIGURES

Figure 1
Effects of shRNA-mediated Mic60 knockdown and rescue in on DA susceptibility differentiated SH-SY5Y cells.
(A) Differentiating SH-SY5Y cells were transfected with empty-vector pRS plasmid (EV-shRNA), GFP-shRNA, or one of three functional Mic60-shRNA vectors (shRNA'05, shRNA'07, shRNA'08). Differentiated cells were collected 72 hr following transient transfection and whole-cell lysate examined by Western blot using Genemed rabbit anti-Mic60. (B) Mic60 levels were quantified from Western blots with respect to the actin loading control in Mic60-shRNA cells (n=4), and GFP-shRNA cells (n=3) and represented as % of EV-shRNA transfection control cells (n=5; mean ± SEM; * = significant from EV-shRNA, p<0.05). (C-E) Cells were treated at 72 hr following transfection. Viability was assessed by trypan blue exclusion following 24 hr treatment with either 250 μM DA or non-treated control media. (C) No difference in basal viability was observed between the transfection control and Mic60-shRNA groups. (D) Following 24 hr treatment, viability was assessed for both DA-treated and non-treated cells, and is represented as % cell death from respective non-treated cells (n=6, mean ± SEM). Cell death was significantly increased in transiently-expressing Mic60-shRNA cells as compared to treated controls (* = significant from DA-treated non-transfected Control and GFP-shRNA, p<0.05; ** = significant from treated EV-shRNA, p<0.05). (E) Differentiated SH-SY5Y cells were co-transfected with one of three combinations: *transfection control*, GFP-shRNA plus pcDNA3 empty vector (GFP-shRNA+pcDNA3, n=3); *knockdown control*, pcDNA3 empty vector plus shRNA-Mic60 (shRNA'05+pcDNA3, n=3); and *knockdown and rescue*, shRNA-Mic60 plus FLAG-tagged mouse-Mic60 (shRNA'05+Mic60-FLAG, n=4). Following 24 hr treatment with 250 μM DA or non-treated control media, viability was assessed by trypan blue exclusion, and is represented as % cell death from the respective non-treated cells (mean ± SEM). Cell death was significantly increased in DA-treated shRNA'05+pcDNA3 cells as compared to DA-treated GFP-shRNA+pcDNA3 cells (* p<0.05), while cell death was attenuated in DA-treated shRNA'05+Mic60-FLAG cells as compared to DA-treated shRNA'05+pcDNA3 cells (** p<0.05) .

Figure 2
Transient overexpression of FLAG-tagged Mic60 in differentiated SH-SY5Y cells.
(A) Differentiated SH-SY5Y cells were collected 72 hr following transient transfection of empty vector pcDNA3 (pcDNA3) or FLAG-tagged mouse Mic60 (Mic60-FLAG), with non-transfected Control cells. Whole-cell lysate was examined by Western blot using Genemed rabbit anti-Mic60. A FLAG-immunoreactive band was detected corresponding to the same molecular weight as the detected Mic60 band. (B) Mic60 levels were quantified from Western blots with respect to the actin loading control in differentiated SH-SY5Y cells, as % of non-transfected Control (n=4, mean ± SEM; * = significant from non-transfected Control and pcDNA3, p<0.05). (C-E) Cells were treated at 72 hr following transfection. Viability was assessed by trypan blue exclusion following 24 hr treatment with either DA or non-treated control media. (C) Basal viability did not differ between non-treated empty vector pcDNA3 and Mic60-FLAG transfected cells (n=6; mean ± SEM). (D) Viability is presented as % cell death as compared to respective non-treated cells following 24 hr treatment with 150 μM DA (n=6; mean ± SEM; * = Mic60-FLAG cell death significant from pcDNA3 and non-transfected Control, p<0.05). (E) Viability is

32

presented as % cell death as compared to respective non-treated cells following 24 hr treatment with 250 μM DA exposure (n=3; mean ± SEM; * = Mic60-FLAG cell death significant from pcDNA3 and non-transfected Control, p<0.05).

Figure 3
Transient overexpression of FLAG-tagged Mic60 in differentiated PC12 cells. (A) Differentiated PC12 cells were collected 72 hr following transient transfection of empty vector pcDNA3 (pcDNA3) or FLAG-tagged mouse Mic60 (Mic60-FLAG), with non-transfected Control cells. Whole-cell lysate was examined by Western blot using T3867 rabbit anti-Mic60. A band corresponding to exogenously-expressed FLAG-tagged mouse Mic60 was observed in addition to endogenous forms of Mic60 in Mic60-FLAG cells. (B) Mic60 levels were quantified from Western blots with respect to the actin loading control, and are represented as % of non-transfected Control (n=6; mean ± SEM; * = significant from non-transfected Control and pcDNA3, p<0.05). (C,D) Cells were treated at 72 hr following transfection. Cell viability was assessed by trypan blue exclusion. (C) Viability is presented as % cell death as compared to respective non-treated cells following 24 hr treatment with 150 μM DA (n=5; mean ± SEM; * = Mic60-FLAG cell death significant from pcDNA3 and non-transfected Control, p<0.05). (D) Viability is presented as % cell death as compared to respective DMSO-vehicle treated cells following 48 hr treatment with 0.5 μM rotenone (n=7; mean ± SEM; * = Mic60-FLAG cell death significant from pcDNA3 and non-transfected Control, p<0.05).

Figure 4
Stable overexpression of FLAG-tagged Mic60 in differentiated SH-SY5Y cells.
(A) Non-transfected passage-matched Control SH-SY5Y cells and stable-expressing Mic60-FLAG, pcDNA3 Empty Vector, and mitoYFP SH-SY5Y cells were differentiated for 5 days, collected, and whole-cell lysate examined by Western blot using T3867 rabbit anti-Mic60. A FLAG-immunoreactive band was detected corresponding to the same molecular weight as Mic60. (B) Mic60 levels were quantified from Western blots with respect to the actin loading control, and presented as % of non-transfected Control cells (n=4; mean ± SEM; * = significant from non-transfected Control, pcDNA3, and mitoYFP, p<0.05). (C-E) Differentiated cells underwent 24 hr treatment with 250 μM DA or non-treated control media (C,D), or 48 hr treatment with 0.5 μM rotenone or DMSO vehicle (E). Viability was assessed by trypan blue exclusion. (C) Basal viability did not differ between empty vector pcDNA3, mitoYFP, and Mic60-FLAG stable transfected cells or passage-matched non-transfected Control cells in non-treated media (n=6). (D) Viability is presented as % cell death as compared to respective non-treated cells following 24 hr treatment with 250 μM DA (n=6; mean ± SEM; * = Mic60-FLAG cell death significant from pcDNA3, mitoYFP, and non-transfected Control cells, p<0.05). (E) Viability is presented as % cell death as compared to respective DMSO-vehicle treated cells following 48 hr treatment with 0.5 μM rotenone (n=6; mean ± SEM; * = Mic60-FLAG cell death significant from pcDNA3, mitoYFP, and non-transfected Control cells, p<0.05).

Figure 5
Effects of Mic60 Knockdown on mitochondrial respiration in differentiated SH-SY5Y cells
Differentiated SH-SY5Y cells were transfected with empty vector EV-shRNA, negative control GFP-shRNA, or Mic60 shRNA shRNA'08. On day 3 after transfection, cells were treated with either DMSO vehicle (A,B,E) or 0.1 μM rotenone (C,D,F) for 24 hr, then assessed for

mitochondrial function via a mitochondrial stress test using a Seahorse XF96 extracellular flux respirometer. (A,C) Oxygen consumption rate (OCR) was normalized to post-analysis immunocytochemical quantification of MAP2 protein levels, and is expressed as (pmol oxygen consumption/min)/MAP2 level. (B,D) The three measurements per stress group (Oligomycin, FCCP, and Rotenone & AntimycinA) were averaged per n for one value of respiration, and then averaged across all experiments. (E-F) Reserve capacity of respiration was calculated for each n from the difference between average basal and average maximal respiration, and then averaged across all experiments. (n=18 for DMSO control, n=12 for 0.1 μM rotenone, from 3 independent experiments; mean ± SEM; * = Mic60-shRNA significant from EV-shRNA and GFP-shRNA, p<0.05)

Figure 6
Effects of Mic60 Overexpression on mitochondrial respiration in differentiated SH-SY5Y cells

Differentiated SH-SY5Y cells were transfected with pcDNA3 Empty Vector or Mic60-FLAG. On day 3 after transfection, cells were treated with either DMSO vehicle (A,B,E) or 0.1 μM rotenone (C,D,F) for 24 hr, then assessed for mitochondrial function via a mitochondrial stress test using a Seahorse XF96 extracellular flux respirometer. (A,C) Oxygen consumption rate (OCR) was normalized to post-analysis immunocytochemical quantification of MAP2 protein levels, and is expressed as (pmol oxygen consumption/min)/MAP2 level. (B,D) The three measurements per stress group (Oligomycin, FCCP, and Rotenone & AntimycinA) were averaged per n for one value of respiration, and then averaged across all experiments. (E-F) Reserve capacity of respiration was calculated for each n from the difference between average basal and average maximal respiration, and then averaged across all experiments. (n=18 for DMSO control, n=12 for 0.1 μM rotenone, from 3 independent experiments; mean ± SEM; * = Mic60 significant from Empty Vector, p<0.05)

Figure 7
Effects of Mic60 overexpression on mitochondrial morphology and mitochondrial fission-fusion dynamics in Differentiated PC12 cells

Differentiated PC12 cells transfected with either (A) pcDNA3 Empty Vector or (B) Mic60-FLAG were imaged via confocal microscopy. (C) Images of Empty Vector and Mic60-overexpressing cells were blinded and assessed based on the appearance of their mitochondrial morphology. Individual cells were categorized as exhibiting either truncated tubular or long tubular mitochondria (n=22 and 27 cells, respectively, from 4 independent experiments; mean ± standard deviation; * = significance between Empty Vector group and Mic60 group, p<0.05). (D) A time series demonstrating an observed mitochondrial fusion (at 430sec) and subsequent fission (at 740sec) in the neuritic projection (dotted outline) of a differentiated PC12 cell transfected with mtDsRed2, PA-mtGFP, and pcDNA3 Empty Vector. (E-G) Neuritic mitochondria in differentiated PC12 cells were assessed for total (E) fission or (F) fusion events per total photoactivated mitochondria (n=80-89 mitochondria from 4 independent experiments; mean ± standard deviation; * p<0.05). (G) Neuritic mitochondria were measured and the individual lengths averaged for all mitochondria from Empty Vector or Mic60-overexpressing cells (n=369 mitochondria per group from 4 independent experiments; mean ± SEM; * p<0.005). (H-J) Axonal mitochondria in rat primary cortical neurons were assessed for total (H) fission or (I) fusion events per total photoactivated mitochondria (n=104 mitochondria from 3 independent

experiments; mean ± standard deviation; * $p<0.05$). (J) Axonal mitochondria were measured and the individual lengths averaged for all mitochondria from Empty Vector or Mic60-overexpressing cells (n=427 and 418 mitochondria, respectively, from 3 independent experiments; mean ± SEM; * $p<0.005$).

Figure 8
Quantification of mitochondrial interconnectivity in differentiated PC12 cells overexpressing Mic60
(A,B) Representative time series of images showing mtDsRed2 and PA-mtGFP fluorescence in (A) Empty Vector and (B) Mic60 transfected differentiated PC12 cells before photoactivation (Pre-Photoactivation), after photoactivation (Post-Photoactivation), and at 20 min intervals following photoactivation. (C,D) Plots of PA-mtGFP fluorescence intensity over time in individual cells transfected with (C) Empty Vector or (D) Mic60-FLAG. (E) Percent decrease in PA-mtGFP fluorescence at 60 min following photoactivation as compared to 0 min Post-Photoactivation. Percent decrease in Mic60 cells was significantly greater than Empty Vector cells (* $p<0.05$, mean ± SEM). (F) Difference in PA-mtGFP fluorescence intensity between scan time points (mean ± SEM). (n = 21 cells for Empty Vector and 26 cells for Mic60, from 3 independent experiments)
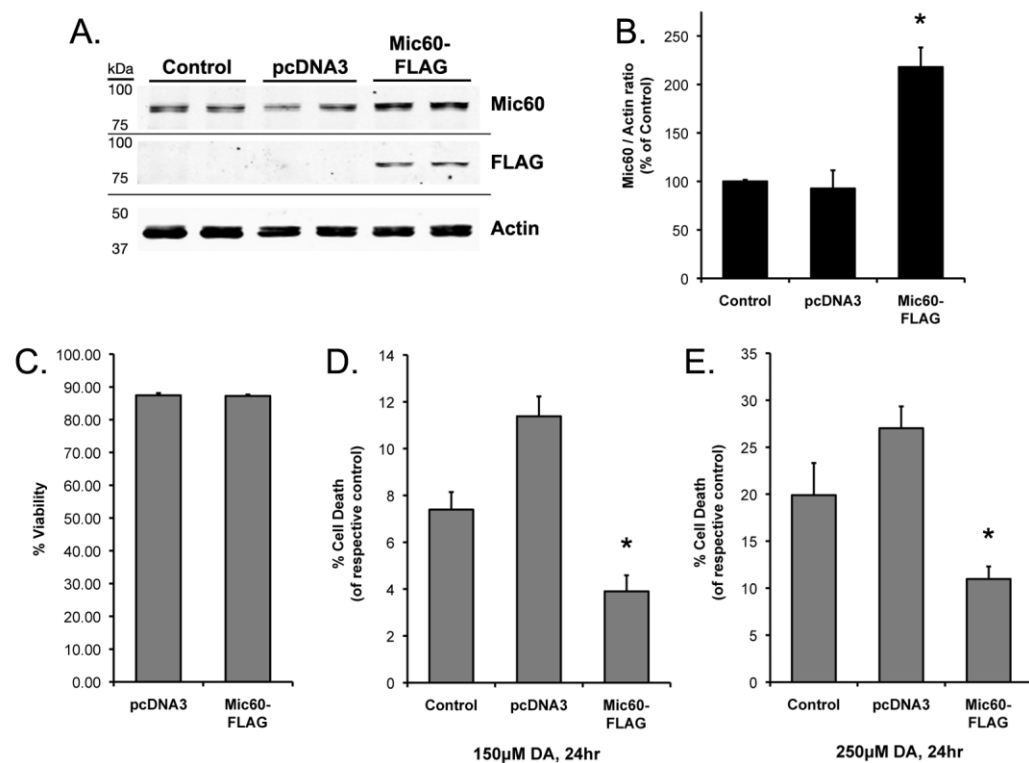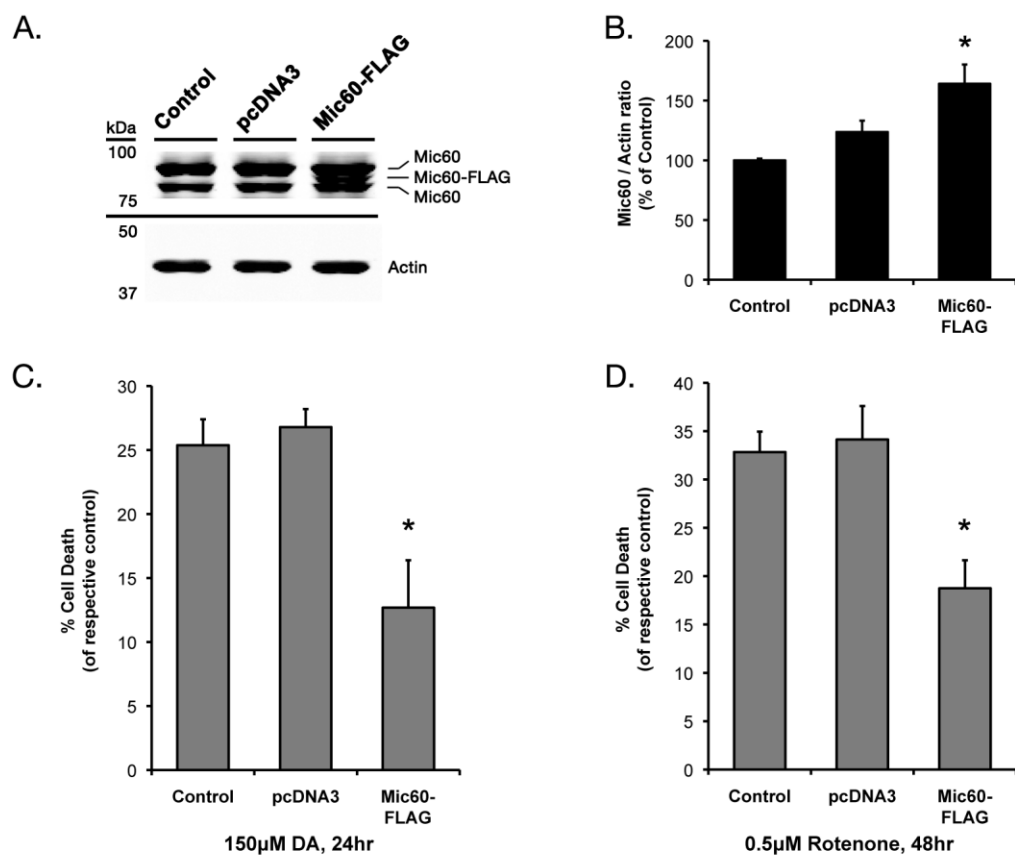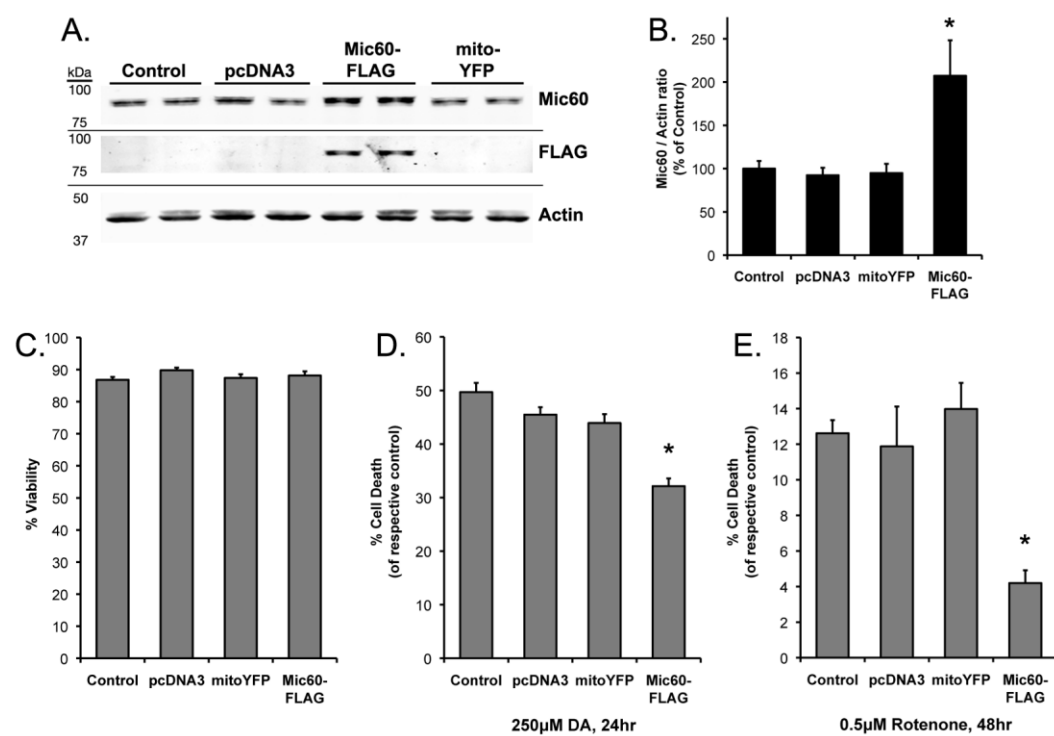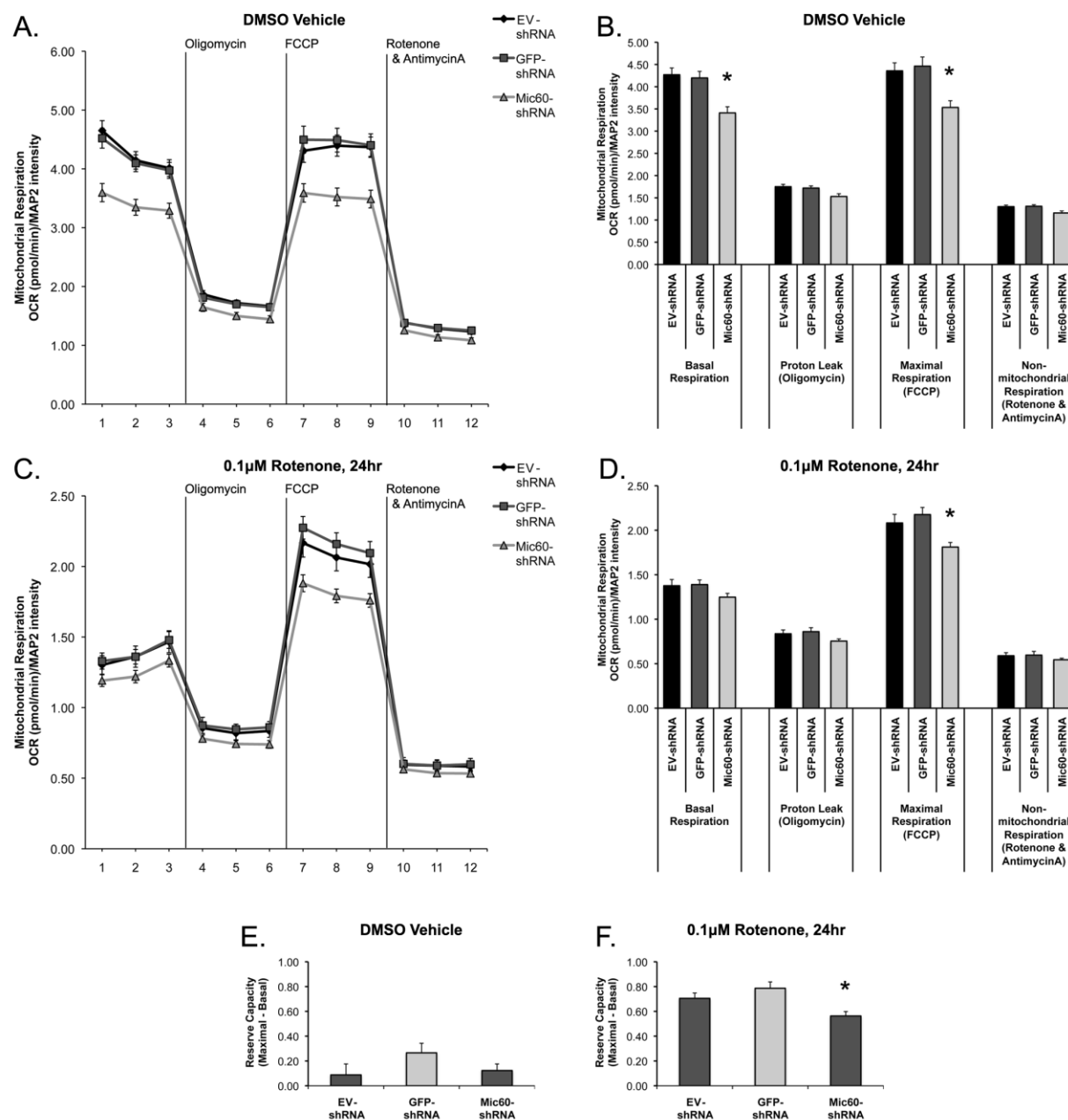
Figure 1

Figure 2

Figure 3
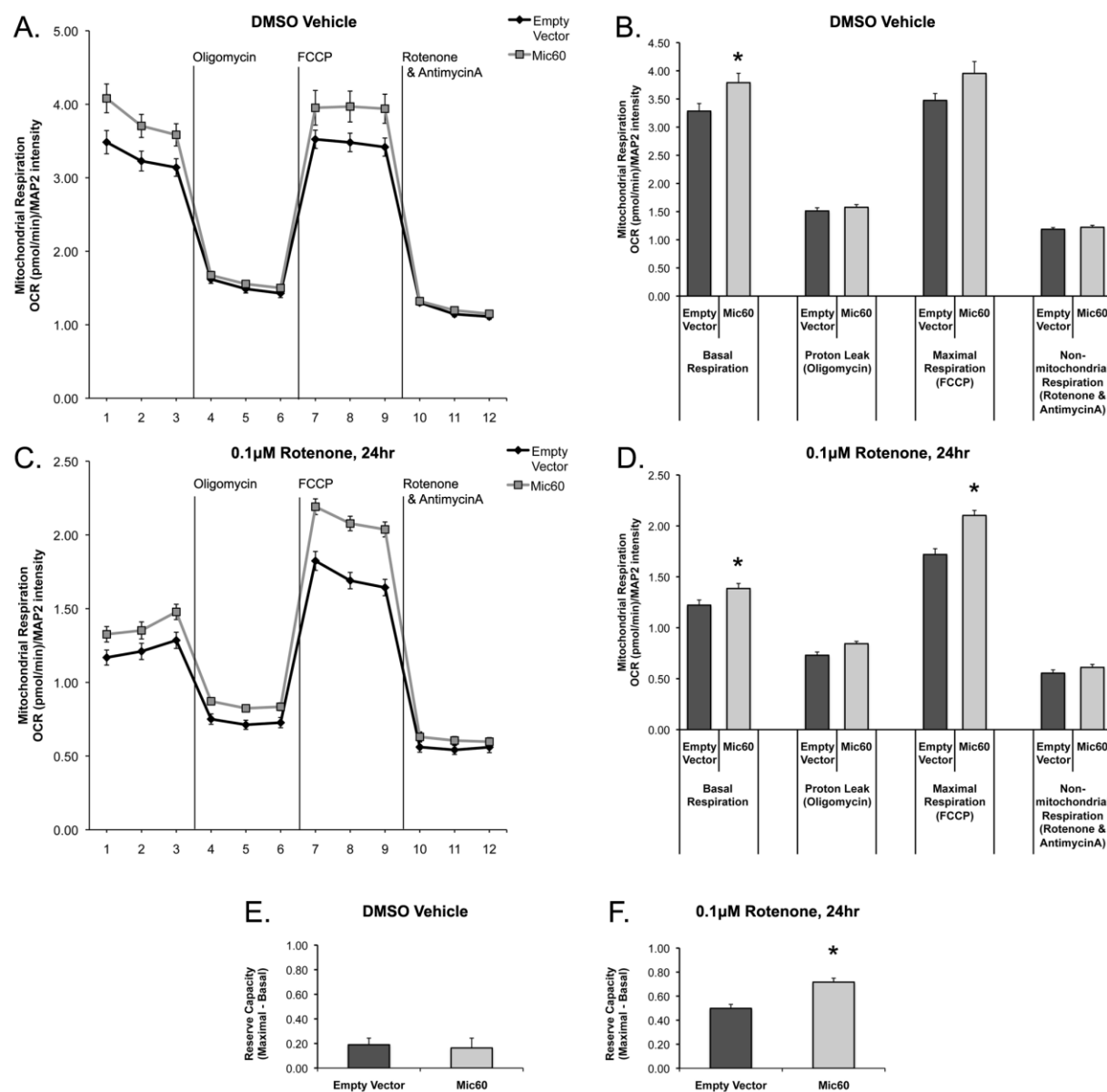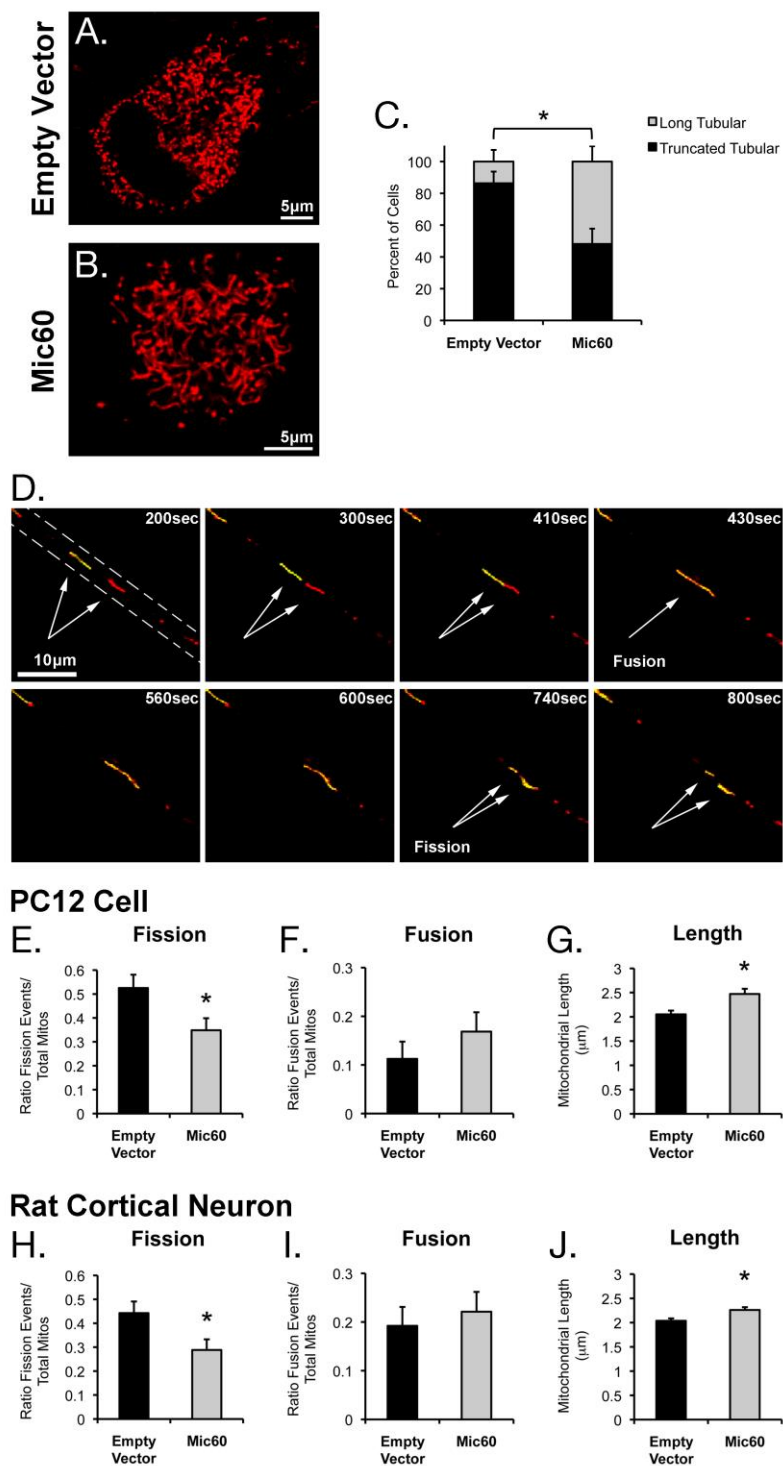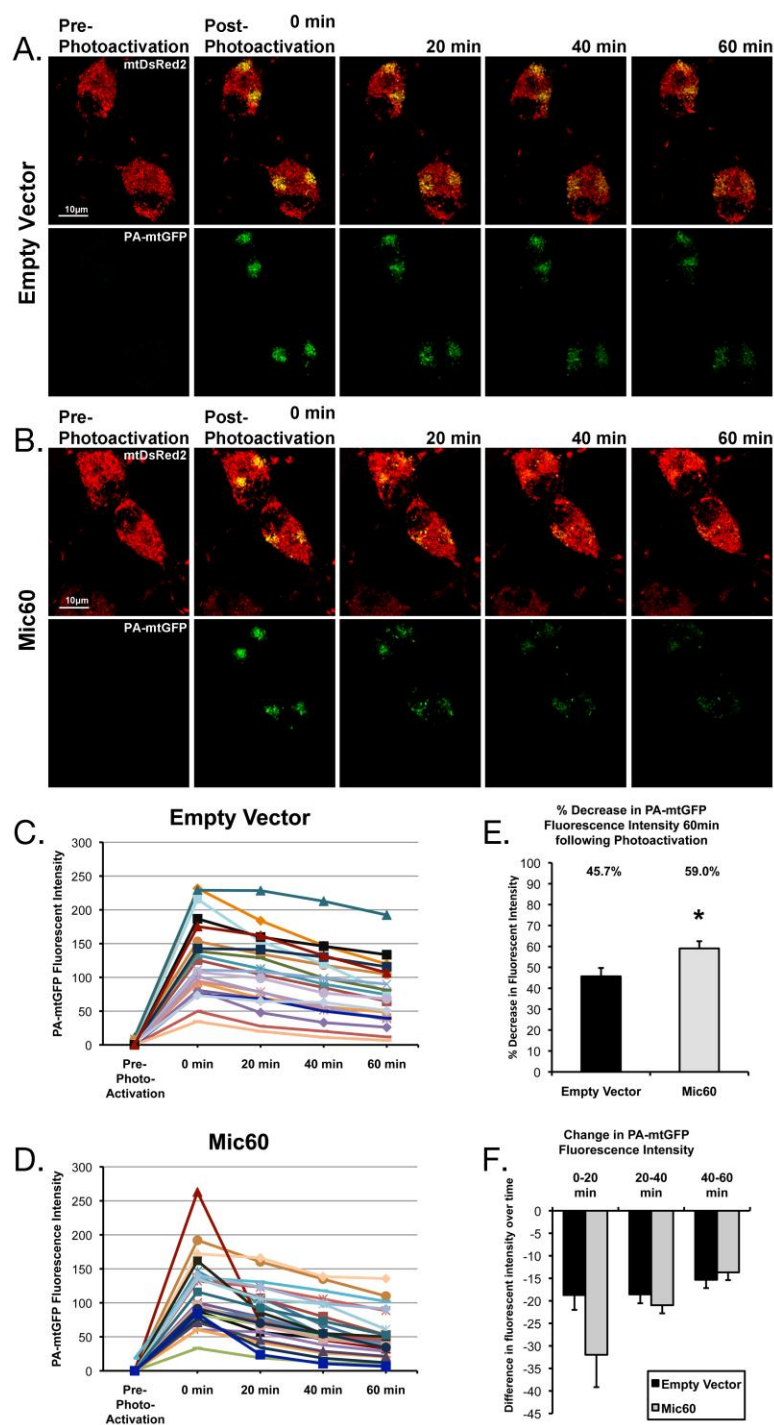
Figure 4

Figure 5

Figure 6

41

Figure 7

Figure 8

Highlights

- The role of mitochondrial mitofilin (Mic60) in cell vulnerability was examined in models of Parkinson's disease (PD).
- Decreased Mic60 expression increased cellular vulnerability to dopamine (DA)-induced toxicity.
- Mic60 overexpression attenuated cellular vulnerability to DA- and rotenone-induced toxicity.
- Cells overexpressing Mic60 exhibited elevated mitochondrial respiration and increased spare respiratory capacity following low-dose rotenone.
- Neuronal cells overexpressing Mic60 displayed suppressed mitochondrial fission and increased mitochondrial length in neurites.